*J. Fluid Mech.* (1993), *vol.* 255, *pp.* 237–274



# The mechanics of gas fluidized beds with an interval of stable fluidization

By S. C. TSINONTIDES AND R. JACKSON
Department of Chemical Engineering, Princeton University, Princeton, NJ 08544, USA

(Received 21 September 1992 and in revised form 8 March 1993)

When small, light solid particles are fluidized by gases it is well known that stable expansion occurs over a finite interval of gas flow beyond the point of minimum fluidization. The existence of such an interval can be predicted from linear stability theory provided the momentum equation for the particles contains a sufficiently large term representing an effective pressure that increases with the concentration of the particles. There is at present some controversy regarding the physical origin of such a term. Some workers attribute it to forces exerted between particles at points of solid–solid contact, while others invoke hydrodynamic mechanisms related to the interaction between the particles and the fluid. In this paper the processes of fluidization and defluidization for fine particles are followed very carefully round complete cycles, starting from zero gas flow and extending to a value at which bubbles appear, then back to zero. The depth of the bed and the pressure drop in the gas traversing it are recorded at each stage, and vertical profiles of the volume fraction of particulate material are determined with a high-resolution gamma-ray densitometer. Similar information is also obtained for sub-cycles extending over more restricted intervals of the gas flow rate. The particles studied are cracking catalyst, with mean diameter 75 μm, and Ottawa sand with mean diameter 154 μm. The results lead to the conclusion that the particle assemblies exhibit yield stresses throughout the range of stable behaviour, and thus are not truly fluidized beds, in the accepted sense. The phenomena observed are such that it is most unlikely that their origin is hydrodynamic. For the particular systems studied we therefore conclude that contact forces are responsible for stabilization.

## 1. Introduction

Figure 1 illustrates the idea of ideal fluidization by plotting the pressure drop of the fluidizing fluid in passing through a particle bed, and the height of the bed, as functions of the fluid flow, expressed as a superficial velocity. As the flow is increased from zero the bed at first remains undisturbed but the pressure drop (and consequently the drag force exerted on the particles) increases and, correspondingly, smaller forces are transmitted at contacts between the particles to support their weight. When the frictional pressure drop reaches the total weight of the particles in the bed (the condition of minimum fluidization) further increase in the flow causes the bed to dilate without any change in the pressure drop. The weight of the particles is then borne completely by the drag forces exerted on them by the fluid, and there is no support from forces of interaction between the particles. If the flow rate is subsequently decreased progressively, these curves are expected to be retraced in detail.

In practice, in contrast to the above picture, when the gas flow exceeds that required for fluidization, gas fluidized beds are observed to be traversed by rising bubbles; that

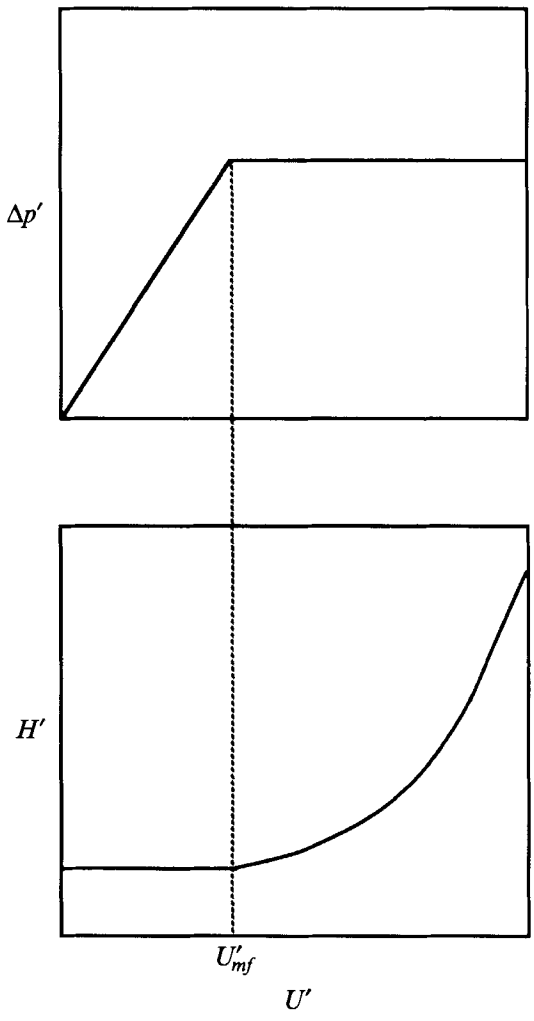


FIGURE 1. Dependence of pressure drop and bed height on fluid flow for ideal fluidization.

is, regions essentially devoid of particles. Bed expansion is now curtailed, and further increases in flow may actually cause a decrease in height. With large, dense particles bubbling begins as soon as the gas flow exceeds that corresponding to minimum fluidization but, for particles of sufficiently small size and low density, there is found to be an interval of gas flow beyond the point of minimum fluidization over which the bed expands in an apparently ideal manner, without bubbling. In his well-known classification Geldart (1973) refers to this class of particles as 'aeratable'. This interval of ideal fluidization is terminated by a 'minimum bubbling' point, beyond which the characteristic pattern of bubbles appears and expansion is curtailed.

The physical origin of this behaviour has been the focus of many investigations. Quite early Jackson (1963) showed that an ideal fluidized bed is always unstable if there are no interaction forces between particles so that they are supported entirely by the drag force, which depends only on the gas flow and the void fraction. The instability takes the form of rising periodic variations in particle concentration, and in typical gas fluidized beds these were found to grow in amplitude very rapidly, so they were tentatively identified with the origin of bubbling. It was not until later that it was

recognized that expansion without bubbling could sometimes occur, and it then became necessary to account for the existence of an interval of stability beyond the point of minimum fluidization. Anderson & Jackson (1968) showed that the inclusion in the equations of motion of viscous stresses, related to the rate of deformation of the particle assembly, did not stabilize the bed, though it did ensure that disturbances grew at a bounded rate and that the dominant disturbances were of finite spatial extent. However, using the stability criterion in the form presented by Wallis (1969), Rietema (1973) showed that cohesive forces between particles in contact could stabilize the system. Later, Garg & Pritchett (1975) recognized that the addition to the particle momentum equation of *any* force proportional to the spatial gradient of the particle concentration will stabilize the bed, provided the magnitude of the force is large enough and it is directed from regions of high concentration to regions of low concentration.

Since then there have been a number of speculations regarding the physical origin of such a force. Mutsers & Rietema (1977*a*), enlarging on the ideas of Rietema (1973), attributed it to cohesive forces exerted at contacts between the particles. In support of this view they demonstrated experimentally that, up to some limiting angle, the free surface of a non-bubbling bed tilts when the axis of the containing vessel is inclined to the vertical, indicating that the assembly of particles has a non-vanishing yield strength. In a second paper (Mutsers & Rietema 1977*b*) they noted that, for given particles fluidized by different gases, the void fraction at minimum bubbling should depend on the ratio $g/\mu$ if theirs is the appropriate stabilizing mechanism, in contrast to a dependence on $g/\mu^2$ if stabilization is hydrodynamic in origin, as originally suggested by Verloop & Heertjes (1970). The results of experiments performed under different effective gravity forces, generated in a large centrifuge, were found to favour the former correlation, and hence support the hypothesis of contact forces. The contact forces were assumed to impart an effective elastic modulus $E$ to the assembly of particles, and in terms of this it was shown that the uniform bed is unstable if

$$\frac{\rho_p^3 d_p^4 g^2}{\mu^2 E} > \left[\frac{150(1-\epsilon)}{\epsilon^2(3-2\epsilon)}\right]^2, \tag{1}$$

where $\rho_p$ is the density of the material from which the particles are made, $d_p$ is the particle diameter, $g$ and $\mu$ are the gravitational acceleration and the viscosity of the gas, respectively, and $\epsilon$ denotes the void fraction. This predicts instability for sufficiently large values of $\epsilon$, so there is an interval of uniform fluidization only if this value of $\epsilon$ is larger than the void fraction at minimum fluidization.

More than a decade after the first publication of Rietema, Foscolo & Gibilaro (1984) emphatically rejected the idea that interparticle forces are responsible for the stabilization of the bed at gas flows below that required to initiate bubbling. Instead they invoked the stability criterion in Wallis's (1969) form, generating an 'elastic wave' velocity by arguing that the gas–particle drag force should contain an additional term proportional to the gradient in the void fraction. This led to a simple criterion for instability of the form

$$\frac{(gd_p)^{\frac{1}{2}}}{v_t}\left(\frac{\rho_p-\rho_g}{\rho_p}\right)^{\frac{1}{2}} < 0.56n(1-\epsilon)^{\frac{1}{2}}\epsilon^{n-1}, \tag{2}$$

where $\rho_g$ is the density of the gas, $v_t$ is the terminal velocity of free fall of a particle in the gas under gravity, and $n$ is the Richardson–Zaki (1954) exponent for the particles in question. The right-hand side of (2) vanishes at $\epsilon = 0$ and $\epsilon = 1$, and passes through a single stationary maximum at some intermediate value of $\epsilon$. If this maximum is

smaller than the left-hand side, the bed is stable for all $\epsilon$; otherwise there is a proper subinterval of (0, 1) over which the bed is predicted to be unstable. Thus there is always a predicted interval of stability for values of $\epsilon$ sufficiently close to unity, and a second interval may also exist immediately after minimum fluidization. The Richardson–Zaki exponent $n$ depends only on the Reynolds number for an isolated particle falling at its terminal velocity, so (2) is an appealingly simple form of stability criterion, for which its authors claim agreement with observation over a wide range of gas fluidized beds, at both atmospheric and elevated pressures, and also for liquid fluidized beds. However, this agreement depends on their identification of the limit of stability with the condition under which visible bubbling first occurs. The two are by no means conceptually equivalent, and a linear stability theory cannot predict whether unstable infinitesimal disturbances will grow into bubbles, as we recognize them, or into something quite different. Indeed, there is independent evidence from different laboratories (Anderson & Jackson 1969; El-Kaissy & Homsy 1976; Homsy, El-Kaissy & Didwania 1980; Ham *et al.* 1990) that certain water fluidized beds of glass beads, predicted to be stable over the whole range of flows by criterion (2), are actually unstable, though the instabilities never grow into bubbles. The last cited workers, making careful observations just above the point of minimum fluidization, detected a very narrow interval of apparently stable behaviour, but this is not consistent with the broad range of stability predicted by the Foscolo–Gibilaro criterion. Furthermore, as will be seen later, the prediction of (2) for the condition of minimum bubbling in a gas fluidized bed studied in the present work is not in good agreement with our observations. Thus, while this criterion has certainly had some success in indicating the relative stabilities of different systems, and in accounting for the effect of gas pressure on stability, we do not believe that the present experimental evidence supports claims for its universal applicability or quantitative accuracy.

A second approach to a hydrodynamic mechanism for stabilization has been proposed by Batchelor (1988), who rejected the contention that stabilization is the result of a dependence of the drag force on concentration gradient. Instead he showed that the stabilizing term could arise from random fluctuations in the particle velocity, and linked it to diffusion of particles within the suspended assembly. His condition for instability, namely

$$\frac{(gd_p)^{\frac{1}{2}}}{v_t}\left(\frac{\alpha}{2(1+\theta)}\right)^{\frac{1}{2}} < n(1-\epsilon)\,\epsilon^{n-1} \tag{3}$$

is quite similar in form to that of Foscolo & Gibilaro, though it contains two factors $\alpha$ and $\theta$, whose values are not immediately known, which are related to virtual mass effects and to the particle phase pressure. Nevertheless, these quantities can be determined, in principle, from independent measurements unrelated to the bed stability, so the criterion is fully predictive.

Controversy regarding the physical reason for the stabilization continues (Rietema & Piepers 1990), but all seem to agree that a term of the form invoked by Garg & Pritchett (1975) is responsible for the observed interval of stable behaviour beyond the condition of minimum fluidization. The proponents of interparticle contact forces argue that hydrodynamic effects cannot generate a term large enough to impose stability, and advance specific experimental evidence of the existence of contact forces, such as the persistence of an inclined surface in a tilted bed and the large value of the effective electric conductivity for stable fluidized beds of small carbon particles. The proponents of a hydrodynamic mechanism of stabilization, on the other hand, argue that, if stabilization were the result of contact forces, the condition of minimum

bubbling would be very sensitive to factors such as the humidity of the gas, which influence the condition of the solid surfaces. They also note that criteria for the existence of an interval of stable fluidization, such as the Geldart classification, do not take any account of such factors.

There is now a great deal of information in the literature about the behaviour of many particulate systems during the transition to fluidization, and thence to bubbling (see, for example, the extensive studies of Abrahamsen & Geldart 1980), but the emphasis has been on covering a wide range of physical properties for the particles and the fluidizing fluid, rather than studying the process in great detail for individual cases. It seems to us, on the other hand, that much can be learned about the nature of the fluidized bed by studying, much more carefully, the way in which a bed expands and recompacts in the processes of fluidization and defluidization. The objective of the present paper, therefore, is to study in some detail the effect of progressive incremental variations in gas flow, both upward and downward, through cycles spanning the whole interval between zero and the bubbling condition, and also through cycles spanning more limited ranges of flow. The investigation is limited to two materials, fluid cracking catalyst and fine sand, with the greatest emphasis on cracking catalyst since this is commercially important, and is commonly regarded as the archetype of materials which exhibit an extended range of stable behaviour when fluidized by a gas. The investigation is in two parts. First the beds are taken through the cycles referred to above, with great care to make successive changes in gas flow in the same direction until the cycle is reversed; the flow control valve is never adjusted back and forth to achieve predetermined increments of flow. At each stage of a cycle the bed height and the pressure drop across the bed are recorded, so these are measurements of the simplest and most conventional kind. In a second phase of the work, the structure of the bed at each stage of expansion and compaction is studied in more detail, using a gamma ray densitometer with very high spatial resolution to determine bulk density profiles.

## 2. Experimental equipment

The ideal system for our purpose would be a fluidized bed of infinite cross-section, equipped with some means to ensure that the fluidizing gas is at all times distributed perfectly uniformly over the lower boundary of the bed. The difficulties encountered in approximating this ideal are well known. In beds of large diameter experience shows that it is very difficult to avoid lateral maldistribution of the gas flow, accompanied by circulation patterns, with particles rising in some places and falling in others. On the other hand, if the diameter is reduced to alleviate this problem, one is concerned that the presence of the bounding walls may influence the observations significantly. The dynamical origin of this dilemma was clarified by Medlin, Wong & Jackson (1974), who showed that uniform fluidized beds, supported above porous distributor plates, are subject to an instability which generates a pattern of motion similar to the well-known convection cells in a fluid heated from below. This instability can be suppressed by using an absolutely uniform distributor whose resistance to gas flow is sufficiently large in relation to that of the bed itself. The necessary resistance increases with the diameter of the bed, but there exists a bounded value of the resistance which, in principle, is capable of eliminating this type of instability in beds of arbitrarily large diameter. In practice, it has always been difficult to devise distributor plates of adequate uniformity and sufficiently high resistance. It is therefore tempting to rely on statistics and use a deep, randomly packed bed of particles as a distributor, but Medlin

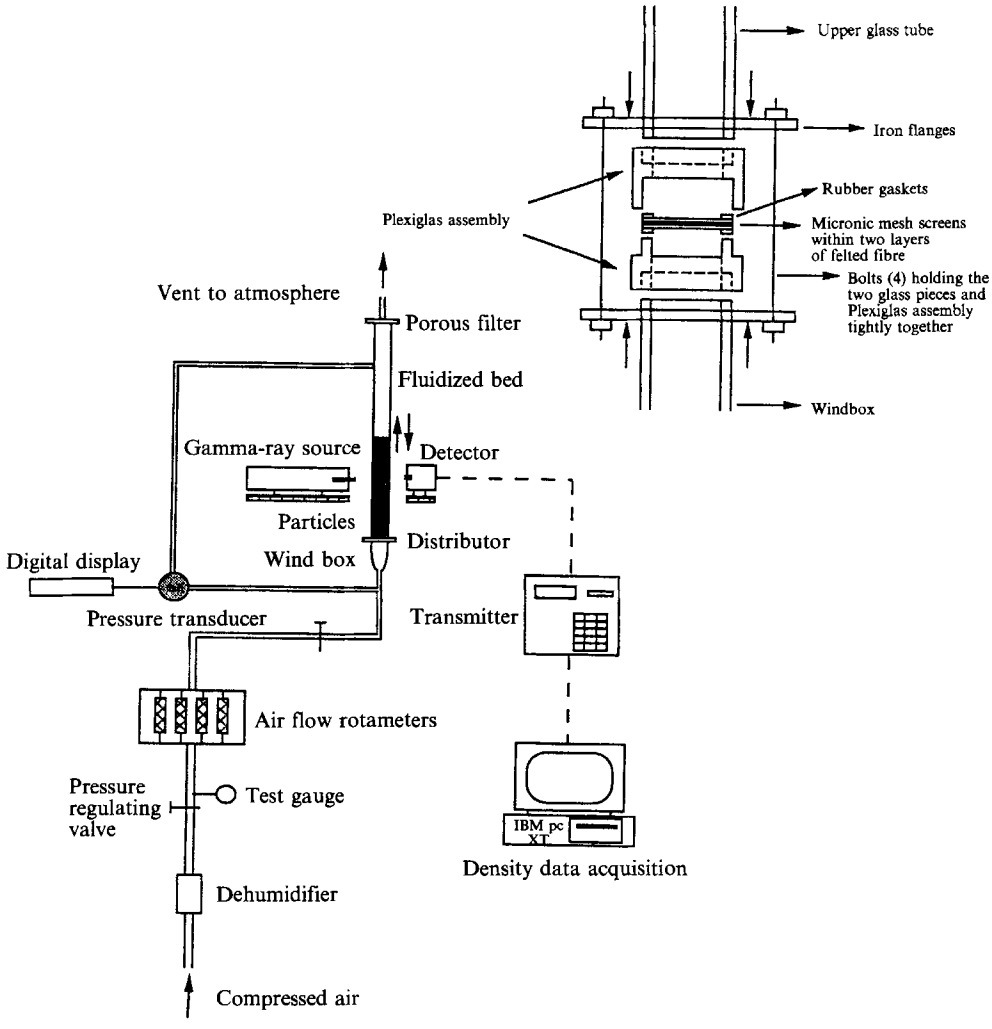


FIGURE 2. Sketch of the apparatus and details of the distributor.

& Jackson (1975) showed that the stabilizing effect is decreased if the resistance is spread over an extended depth. Despite the emergence in recent years of materials such as precision micronic mesh screens and porous plastic sheet, it remains a serious problem to devise an adequate distributor for a large-diameter fluidized bed. We suspect that a number of phenomena with significant implications of principle, such as those reported here, have been obscured in earlier work by consequences of gas maldistribution.

In the present work the beds were formed in glass tubes of two different diameters (1 in and 2 in nominal diameters; actual internal diameters 2.53 cm and 4.99 cm) to assess the influence of the tube walls on the observations. The distributors consisted of two layers of micronic mesh screen (hole size 5 μm) with two layers of felted fibre, each 2 mm thick, sandwiched tightly between them. They were mounted in a Plexiglas housing between the bed and a windbox, which was 10 cm long and had a diameter equal to that of the bed. With this arrangement there was no visible circulation, or preferential points of bubbling, under any of the conditions studied.

The layout of the experimental system is shown schematically in figure 2, with an

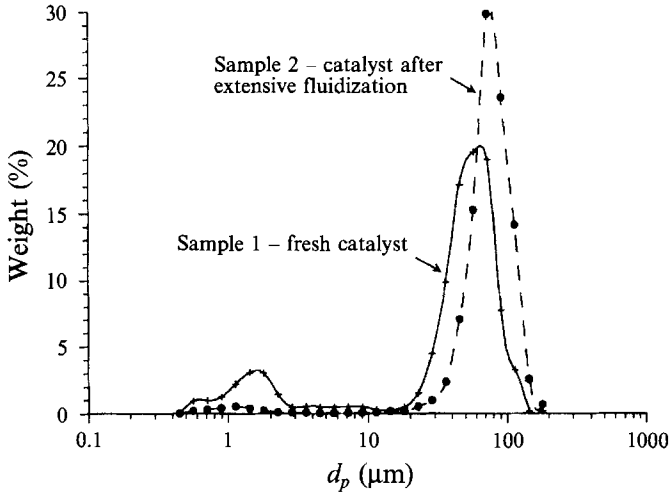


FIGURE 3. Size distributions of the fluid cracking catalyst, both before and after the programme of experiments.

inset giving details of the construction of the distributor. The tubes containing the fluidized beds were approximately 0.9 m long and were closed above by porous filters to catch particles elutriated in the fluidizing air. Air was supplied at 100 p.s.i. by our laboratory compressor. After refrigerated drying and filtration it was let down through a pressure regulator to an adjustable pressure in the range 15–20 p.s.i. The flow to the bed was measured by rotameters and controlled by a valve between the rotameters and the windbox. The pressure at the inlet to the rotameters was monitored by a gauge with precision of 0.1 p.s.i., and was maintained constant throughout the measurements. For high flow rates (300–4000 ml/min) the rotameters were calibrated against a wet test meter, while for low flow rates (0–400 ml/min) they were calibrated against a bubble tube meter. In some tests humid, rather than dry air was used, obtained by bypassing the dryers and bubbling the air through water.

The depth of the bed was determined by a measuring tape attached permanently to the wall of the confining tube. Pressure taps were provided in the windbox and near the top of the tube containing the bed, and the pressure difference was registered by a transducer which had been calibrated against a U-tube manometer containing red oil (specific gravity 0.827). The accuracy of the bed height measurement was estimated to be 0.5 mm, and that of the pressure drop was 1 mm of red oil. The error in the flow measurement was estimated to be less than 0.5 % throughout the entire range spanned in the experiments (0–3500 ml/min). The pressure drop in the freeboard above the surface of the bed was expected to be very small in all the conditions studied, and the pressure drop across the distributor was determined, as a function of the gas flow rate, in separate tests on the empty tube. These were repeated after the experiments on the beds, and the distributor pressure drop was found to be unaltered. The pressure drop across the bed itself was found by subtracting the predetermined distributor pressure drop from the measured overall pressure drop.

Most of the measurements were made on beds of fluid cracking catalyst, though a smaller number of tests used an Ottawa sand of nominal diameter 154 μm. Figure 3 shows the size distribution of the catalyst, both before the start of the work and after several months of testing, during which it had been subjected to many fluidization–defluidization cycles. Over the period of the experiments there is seen to be

some sharpening of the distribution and increase in the mean size, from 54 to 75 μm (these are mass-mean diameters, defined by $d_{ma} = \Sigma x_i d_i$, where $x_i$ is the mass fraction with diameter $d_i$.) A small peak initially present in the 1–2 μm range is eliminated, as would be expected, but caution is needed in interpreting features of this kind, bearing in mind that the size distribution was determined by a Coulter counter technique. The fluidization cycles never expanded the beds much beyond the point of initial bubbling, and most of the time was spent with the bed in a non-bubbling condition. Furthermore, there was no evidence of any change in the cycles throughout the period of the tests. We therefore believe that most of the loss of finer particles occurred when the material was first fluidized, and the measured final size distribution is probably representative of the content of the bed in the bulk of the tests. As further evidence of this, before each series of tests the weight of the material charged to the bed was determined to within 0.01 g. The material remaining in the bed at the end of the series was also weighed and, with dry air, in no case was the loss in weight found to exceed 0.1 % of the weight initially charged. Detailed size distributions were not obtained for the Ottawa sand, but microscopic examination showed the particles to be smooth in shape, more nearly spherical than the cracking catalyst, and narrow in size distribution.

For the experiments with dry air the bed was aerated, at a low flow rate, for at least four hours before starting the measurements, to be sure the particles were free of excess moisture. No obvious symptoms of static electricity were observed in the tests, such as adhesion of particles to the walls of the confining tube, and all the quantitative measurements were very reproducible, so we believe that electrostatic effects were not important. Furthermore, the characteristic and interesting features observed in the experiments with dry air were actually enhanced when humid air was used, showing that they could not have been artifacts of static electricity. Before initiating measurements with humid air the bed was pre-aerated for 12–36 hours to permit the particles to come to equilibrium with the water vapour in the air. The difference between the weight of material discharged after the tests and the weight initially charged gives a measure of the amount of water taken up by the particles.

When the above preliminaries were complete an experiment was initiated by first taking the bed through several complete cycles, from zero gas flow to a flow beyond the point of minimum bubbling, and back again to zero flow. After the completion of the first cycle no systematic changes were observed from cycle to cycle. The test cycle itself was then started from a flow beyond the point of minimum bubbling. The flow was reduced progressively, in small increments, until it reached zero, taking care that all adjustments were made in the direction of decreasing flow rate, and that the bed was not disturbed mechanically in any way. Then, starting from zero, the flow was increased progressively by similar small increments, through the conditions of minimum fluidization and minimum bubbling, and back to the value from which the cycle started. After each change in gas flow the bed was allowed ample time to settle to its new configuration, then the bed height and the pressure drop were measured, and the appearance of the bed was observed and recorded. In the case of any accidental mechanical vibration, or other disturbance, the whole cycle was re-started. As described later, measurements were also made for certain sub-cycles, in which the direction of the increments in gas flow was reversed before the flow had reached zero, or the value that formed the upper limit of the complete cycles. Each type of cycle was repeated several times, and complete cycles and sub-cycles were traversed in random order so as to check the reproducibility of the results.

In addition to the simple measurements of bed height and pressure drop, the structure of the bed at various stages of a fluidization–defluidization cycle was studied

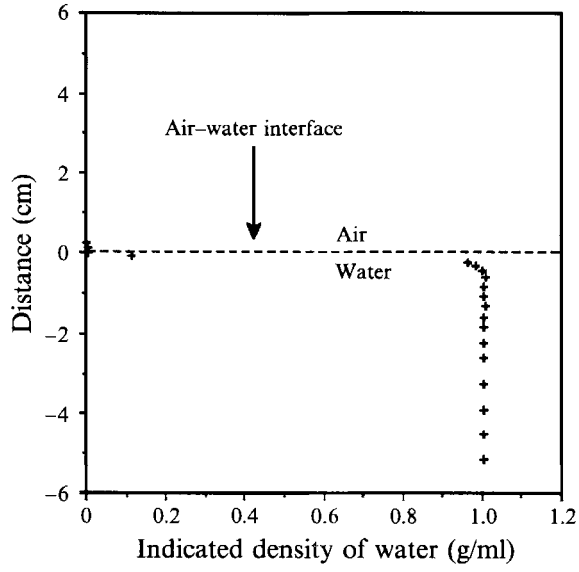


FIGURE 4. Measured density profile for a column of water, as a test of the accuracy and spatial resolution of the densitometer.

in more detail by measuring profiles of the time-average bulk density, using a gamma-ray densitometer. This is indicated in figure 2. Gamma-ray densitometry is used in industry, and instruments, comprising a source and a scintillation detector, are available commercially. For a given material the attenuation of a transmitted beam of gamma rays depends on the total mass of the material encountered along the path of the beam. Therefore, if the density of the material is uniform, its value can be deduced by measuring the unscattered radiation which emerges in the direction of the incident beam. The measurement of the emergent intensity by a scintillation detector is statistical in nature, since the detector counts discrete events, namely the arrival of unscattered photons. The corresponding uncertainty in the measured density can be reduced by increasing the intensity of the source, or extending the interval of time over which the measurement is made, both of which increase the total number of photons counted. Commercial densitometers achieve a satisfactory count rate by using large sources, screened so as to generate an incident beam of quite large diameter. As supplied they are, consequently, unsuitable for investigating the detailed structure of our beds, for which purpose their spatial resolution is quite inadequate. We therefore modified a commercial densitometer to reduce radically the diameter of the radiation beam from the source, aiming for a spatial resolution of a few millimetres.

The commercial instrument consisted of a 500 mCu, Cs-137 source, completely enclosed and shielded except for a shutter which could be opened to allow a gamma-ray beam of 1 in. diameter to emerge, together with a scintillation detector capable of accepting a beam of this diameter. We modified this by mounting lead plates, 2.25 in. thick, in front of the source and the detector. A $\frac{1}{16}$ in. diameter hole drilled through each plate was centred on the axis of the beam. Thus, the source was stopped down to produce a well-collimated beam of approximately $\frac{1}{16}$ in. diameter, while the corresponding hole in front of the detector ensured that only unscattered radiation from this beam could reach the sensitive surface. If collimation were perfect this arrangement would give a spatial resolution of about 1.6 mm, but of course the rate of arrival of photons at the source is greatly reduced compared with that of the original

instrument and, correspondingly, it is necessary to accumulate them for a longer time to achieve the same precision in the value of the density. It is also vital to achieve, and maintain accurate alignment of the two collimating holes, which are to be placed facing each other, on opposite sides of the fluidized bed. In view of the considerable weight of the source, detector, and their associated lead screening, it is extremely difficult to maintain the source and detector in precisely the correct relative position and orientation while, at the same time, mobilizing them as a pair so that they can scan the bed to determine the density distribution. This problem was overcome by mounting them in fixed positions, properly aligned, on an immovable optical table formed from stout aluminium I-beams. The fluidized bed, which was much lighter than the measuring system, was then mobilized by mounting it on the table of an old milling machine, so that the traverses of the mill could be used to move the bed, vertically or horizontally, between the source and the detector. This arrangement proved entirely satisfactory provided the bed was moved very slowly and evenly, using the lead screws of the mill, to avoid disturbing it mechanically.

The measurements were directed mainly to determining the vertical density profile of the bed on a plane containing its axis of symmetry, though a smaller number of runs was devoted to density variations within a given horizontal section. The calibration procedure needed to make the instrument generate directly the vertical density profiles was quite elaborate, and is described elsewhere by Tsinontides (1992). All densities found in this way are, of course, time averages over the length of a period during which counts are accumulated in the detector.

To check the precision and spatial resolution of the modified densitometer the fluidized bed was replaced by a glass tube partly filled with water, and the axial density profile was measured. This is shown in figure 4. With a measuring time of 15–20 min the value of the density at any point below the surface of the water was reproducible to better than 1 % in a number of independent measurements. Correspondingly, the points in figure 4 below the water surface differ from the actual density of water, 0.998 g/cm$^3$, by no more than 1 %. On approaching the plane of the surface from below, the measured density has dropped to 0.96 g/cm$^3$ when the centre of the beam lies 0.25 cm below the surface, a decrease of less than 4 % from the bulk value, then there is a very rapid fall as the centre of the beam is raised through the plane of the surface. Since the actual surface can be regarded as a true discontinuity in density, these results indicate a spatial resolution of about 3 mm; larger than, but of the same order as, the diameter the beam would have it if were perfectly collimated.

## 3. Results of bed expansion and pressure drop measurements

Figures 5 and 6 show measured bed heights and pressure drops for cracking catalyst carried through a complete defluidization–refluidization cycle, starting from a gas flow large enough to generate a freely bubbling bed. The fluidizing medium is dry air, and figure 5 corresponds to a bed contained in the nominal 1 in. diameter tube, while figure 6 refers to a bed in the 2 in. tube. The mass of catalyst loaded, per unit cross-sectional area of the tube (namely 35.7 g/cm$^2$), is the same in both cases and corresponds to an unexpanded bed depth of about 40 cm. Figures 7 and 8 show corresponding results for fluidization with humidified air. In each case the pressure drop is expressed as a multiple of the weight of the catalyst loaded, per unit cross-sectional area of the bed, so when $\Delta p = 1$ the pressure drop exactly balances the weight of the catalyst loaded into the bed. For fluidization with dry air this weight is the same as the weight of catalyst present in the experiments, but for humid air the weight of the catalyst at the

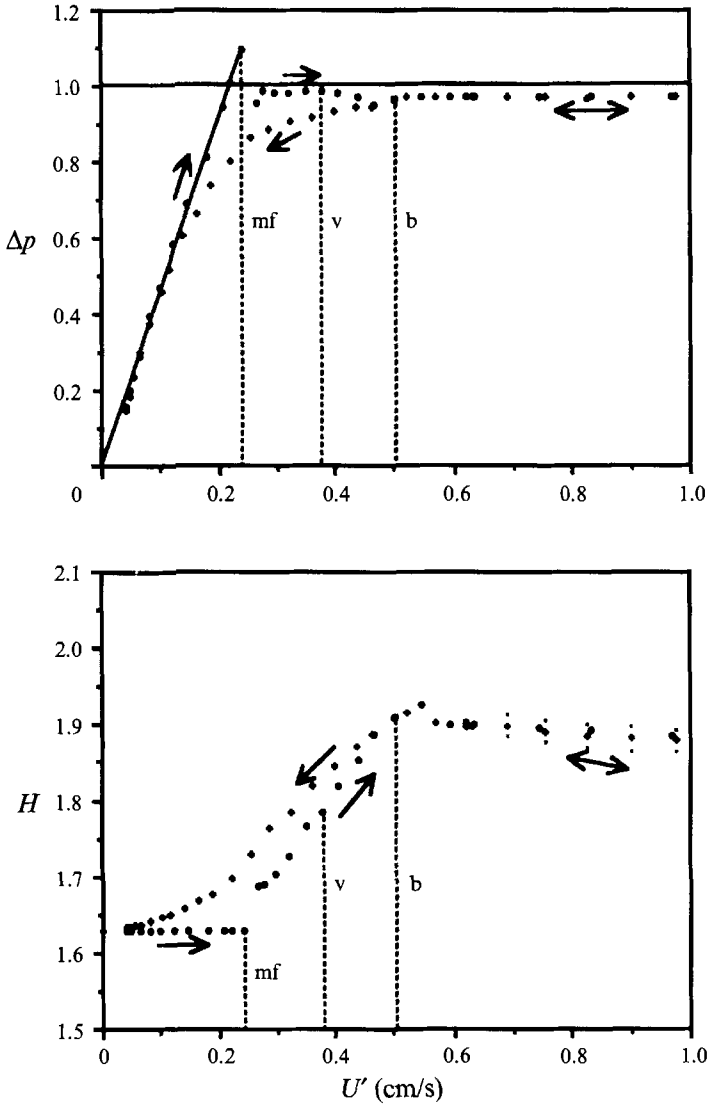


FIGURE 5. Dimensionless pressure drop and bed height, as functions of the gas superficial velocity, for cracking catalyst fluidized by dry air in the bed of nominal diameter 1 in.; ●, increasing gas flow; +, decreasing flow, while 'mf' denotes minimum fluidization, 'b' initiation of bubbling, and 'v' volcanoes (see text).

time of the experiments is larger by the weight of water absorbed from the fluidizing air. (The horizontal lines on the graphs of $\Delta p$ in figures 5–8 show the value of the pressure drop which matches the weight of catalyst in the bed at the time of the measurements, so they lie at $\Delta p = 1$ for dry air, but above $\Delta p = 1$ when the fluidizing air is humidified.) The bed height is given as a multiple of the height that the solid material would occupy if it could be packed into the tube with no voids between the particles, and the gas flow is quoted as a superficial velocity based on the cross-section of the empty tube. Thus

$$\Delta p = \frac{\Delta p'}{mg}; \quad H = \frac{H'\rho_p}{m}; \quad U' = \frac{Q'}{A}, \tag{4}$$

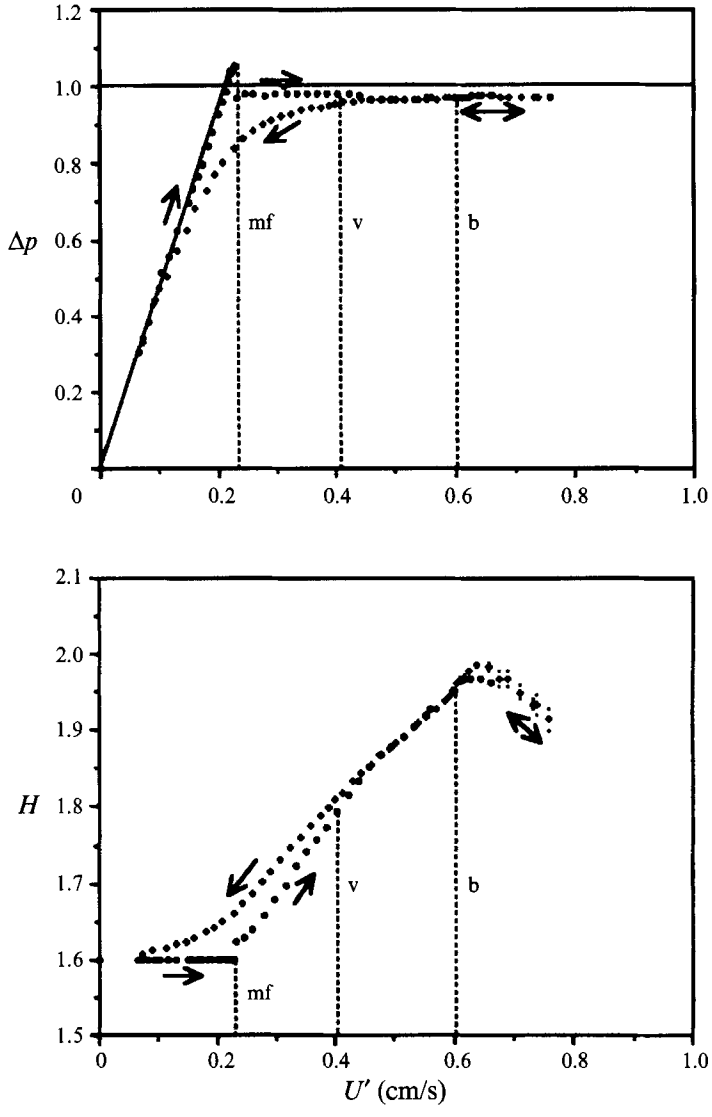


FIGURE 6. As figure 5 but for a bed of nominal diameter 2 in.

where primes distinguish the dimensional pressure drop and bed height, and the total volume flow rate, $m$ is the mass of catalyst loaded, per unit cross-sectional area of the bed, $\rho_p$ is the density of the material from which the particles are formed, and $A$ is the cross-sectional area.

The results are qualitatively similar in all cases, and it must be emphasized that each pair of curves is completely reproducible, in quantitative detail, even if the experiments are separated in time by days and other experimental runs have been made in between. In the bubbling bed the upper surface oscillates and is ill-defined, and this is indicated in the figures by bracketing each point representing the mean bed height by two smaller points, indicating the upper and lower bounds of motion of the surface. The bubbling generated no detectable oscillations in the pressure drop.

The results for increasing values of the gas flow are familiar, and have often been described. Starting from zero flow the pressure drop increases in proportion to the flow

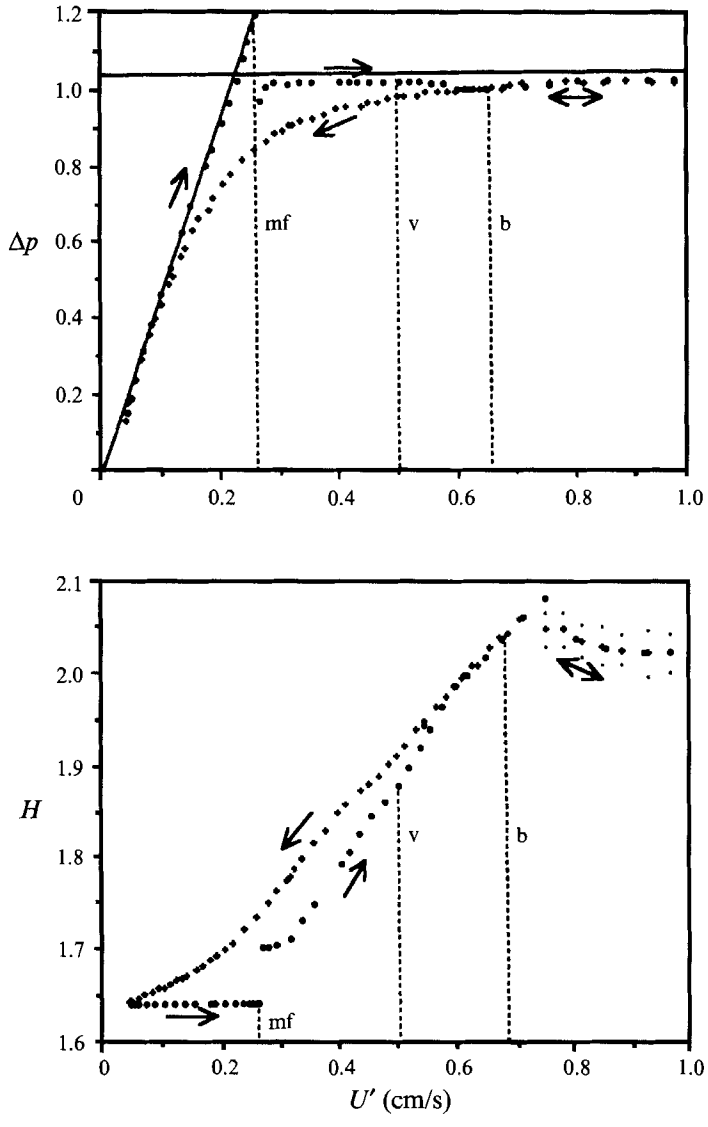


FIGURE 7. Dimensionless pressure drop and bed height, as functions of the gas superficial velocity, for cracking catalyst fluidized by wet air in the bed of nominal diameter 1 in.; ●, increasing gas flow; +, decreasing flow.

rate and the bed height remains constant up to the point of 'minimum fluidization', where bed expansion begins. For a cohesive material, such as cracking catalyst, the pressure drop overshoots beyond the weight of the particle bed before expansion begins, then there is a sudden decrease in the pressure drop and corresponding jump in the bed height as expansion is initiated. There is then a very short interval over which the bed expands only slowly, and the pressure drop increases again to a value not far below the weight of the bed. With further increase in gas flow the pressure drop remains constant, at a value a little below the weight of the bed, while the bed height increases steadily. Finally, the pressure drop decreases by a small, but appreciable amount and, shortly after, visible bubbling begins. The initiation of bubbling is identified by a letter 'b' in the figures. Shortly beyond the point of minimum bubbling

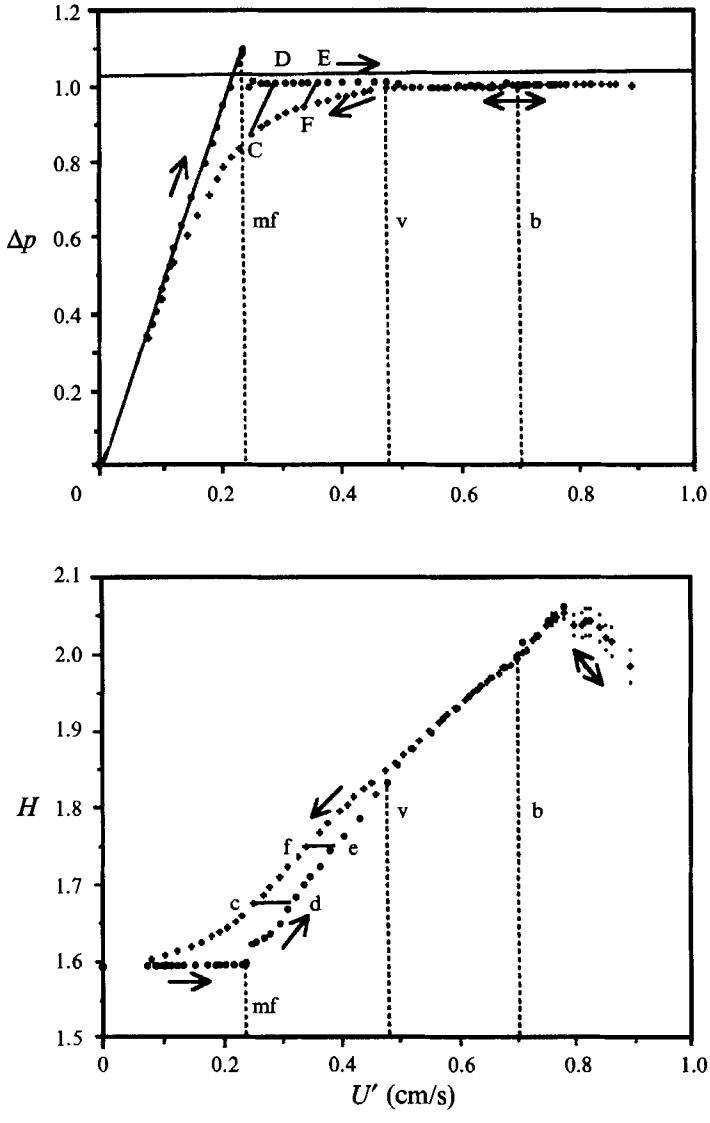


FIGURE 8. As figure 7 but for a bed of nominal diameter 2 in.

the bed height passes through a maximum, then the mean height begins to decrease slowly, with marked oscillations of the free surface as bubbles burst.

When the gas flow is reduced progressively, by small increments, from an initial value in the free bubbling range, the behaviour is quite different. The pressure drop curve lies well below that for increasing gas flow, while the bed height curve lies above that for increasing flow, and neither curve shows any evidence of the 'minimum fluidization' phenomenon so typical of the results for increasing flow. Instead both curves drop smoothly to the values corresponding to zero flow. Thus, there is a very marked hysteresis between the experimental measurements for increasing and decreasing gas flows. The curves for increasing and decreasing flow separate visibly from each other at a value of the gas flow rather less than that corresponding to the initiation of bubbling, and bubbling ceases with decreasing flow at approximately the same flow rate as it began with increasing flow.

The separation of the curves for increasing and decreasing flow is somewhat more marked in the bed confined within the tube of smaller diameter. Similarly, the overshoot in pressure drop, and the corresponding jump in bed height at the point of minimum fluidization, are larger for the tube of smaller diameter. The gas flow for minimum fluidization is not affected appreciably by the diameter of the confining tube, but the interval of flow over which the bed does not bubble is appreciably wider for the tube of larger diameter. With moist air the jumps in pressure drop and bed height at minimum fluidization are larger than with dry air, and moist air also gives a wider interval between minimum fluidization and the onset of bubbling.

Within the interval between minimum fluidization and minimum bubbling there is another visible phenomenon which should be mentioned. As pointed out above, for increasing gas flow there is an interval just before minimum bubbling over which the pressure drop falls slightly as the gas flow increases. For flows within this interval there are observed to be intermittent, local eruptions of particles at random points of the bed surface. Each eruption leaves a small cone of solid material at the surface when it subsides, so we have named them 'volcanos'. The lowest gas flows at which volcanos appear are identified by the letter 'v' in the figures.

The major feature of these results is the hysteresis between the measurements of pressure drop and bed height for increasing and decreasing gas flows. This strongly suggests the existence of yield stresses in the particle assemblies which form the expanded, but non-bubbling beds. Consider, for example, the corresponding points identified by upper-case letters on the pressure-drop plot of figure 8, and by the same lower-case letters on the bed-height plot. Then points C, c and D, d correspond to beds of the same height, and hence particle assemblies of the same average bulk density. However, at D the pressure drop almost matches the weight of the bed, so only small forces are transmitted through the particle assembly, whereas at C the pressure drop is substantially less than the weight of the bed, so the particles must derive a significant fraction of their support from forces transmitted through the assembly to the distributor (through which the gas enters) and to the lateral bounding walls. If this simple interpretation is correct, starting with the bed in the condition represented by point C, it should be possible to increase the gas flow progressively, thus increasing the drag force on the particles and reducing the support they must derive from mutual contact, without causing any change in the bulk density or the structure of the particle assembly until a pressure drop beyond D is reached, at which cohesive forces are overcome and the bed expands. Throughout this process, as long as the bed structure remains unchanged, points representing the pressure drop should lie on the straight line segment joining C to D and this should pass through the origin when extrapolated. An experiment of this type will be referred to as a partial fluidization cycle of type 1, or a PC-1 cycle for brevity. Similarly, starting with a bed in a condition represented by a point such as E, if the gas flow is reduced progressively there should be no change in the bulk density or bed structure until point F is reached, and points representing the pressure drop should lie on the line segment EF which, when extrapolated, passes through the origin. This will be referred to as a PC-2 cycle. In either of these experiments the bed height should remain unchanged, following the horizontal line segments cd or ef, respectively, in the bed-height plot.

Figure 9 shows the results of PC-1 experiments in the bed of catalyst fluidized by dry air in the 2 in. nominal diameter tube. Each experiment started from the freely bubbling bed, and the gas flow was reduced successively to reach points A, a and B, b, respectively, in the two experiments. The flow was then increased again in small increments, and it is seen that the measured values of the pressure drop fell, with great

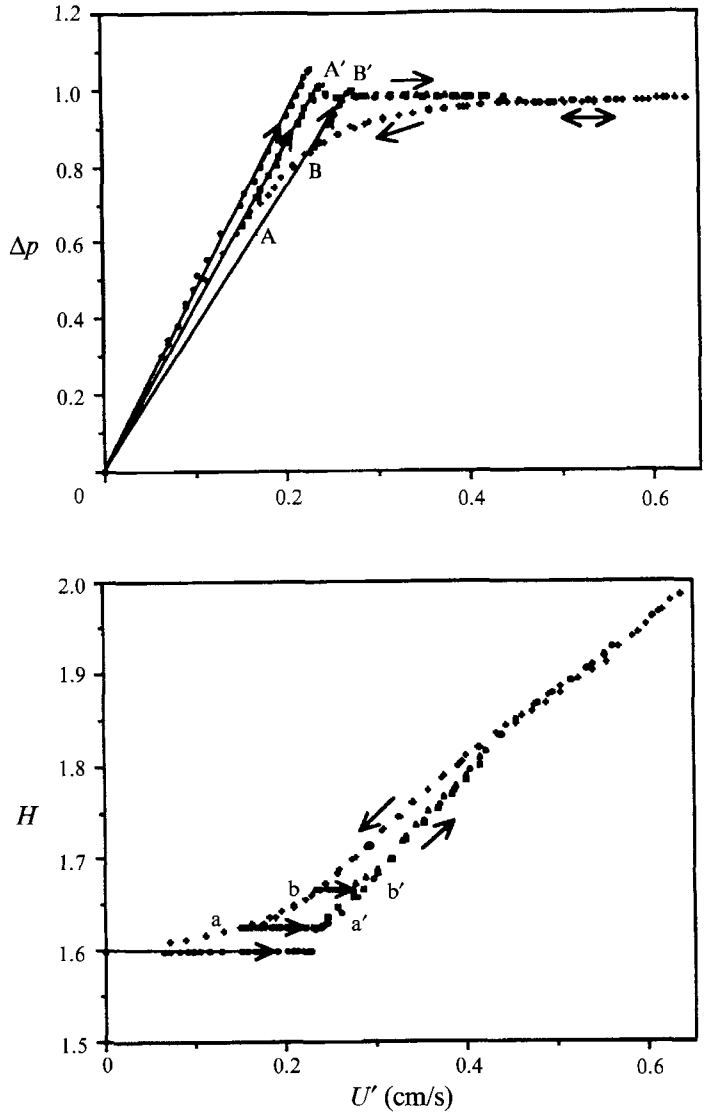


FIGURE 9. PC-1 cycle for cracking catalyst fluidized by dry air in the bed of nominal diameter 2 in.; □ denotes points obtained by increasing the gas flow, starting from a partially compacted bed.

precision, on the straight lines joining the origin to points A and B, respectively, as predicted. At the same time, the measured bed heights remained unchanged. Before any expansion occurred the pressure drop exceeded the bed weight, and it is seen that the amount of overshoot needed to initiate expansion became smaller as the bulk density of the particle assembly was reduced; thus the overshoot at minimum fluidization was larger than the overshoot at point A′, which was in turn larger than the overshoot at point B′. This is just what would be expected if the cohesive yield strength decreases, as it should, when the bulk density is decreased. These simple experiments showed only that the overall bulk density of the particle assembly remains unchanged on AA′ and BB′, but gamma-ray density scans (described later) revealed also that the detailed structure of the assembly was completely invariant along these

segments. The implication of these results needs to be emphasized. A segment such as AA′ contains a point at which $\Delta p = 1$ where the pressure drop exactly balances the weight of the particles, and there are no supporting stresses transmitted through the assembly. Such an assembly might, therefore, be regarded as a fluidized bed. However, the *same* assembly at point A is capable of transmitting a quite substantial compressive stress without any change in structure. This is not a feature of a classical fluidized bed. The same behaviour is found in the beds fluidized in the narrower tube, and with moist air in tubes of both sizes (see Tsinontides 1992) so these results are not peculiar to this particular experimental configuration.

The curve of pressure drop versus gas flow, traced during a conventional fluidization experiment, in which the flow is increased progressively from zero, is also shown in Figure 9. It crosses the line segment BB′ and, at the crossing point, it is a horizontal line corresponding to a pressure drop only slightly less than the bed weight. The beds represented by these coincident points on the horizontal curve for fluidization starting at zero flow, and on the line segment BB′, are quite different in structure and properties, though they have the same overall expansion. Thus, if the direction of successive changes in gas flow is reversed at this point of BB′, the sequence of observed states simply retraces its steps down BB′ toward B. However, successive decreases in gas flow from the coincident point of the increasing flow curve constitute a PC-2 experiment, as defined above, and the observed behaviour is radically different.

We therefore turn to the experiments on PC-2 cycles. The behaviour in these cycles is again found to be qualitatively the same in tubes of different diameter, and with both moist and dry air (Tsinontides 1992), so we present here in figure 10 only the measurements for fluidization with moist air in the nominal 2 in. diameter tube, since the rather complicated behaviour is most easily seen in these results. The bed was first defluidized progressively from the freely bubbling state (plusses in figure 10), then partially refluidized to a point within the interval between minimum fluidization and minimum bubbling (triangles in the figure), and finally defluidized progressively once more (circles in the figure). In the final defluidization process our simple argument above suggested that the pressure drop should initially retreat along a straight line through the origin, while the bed height should remain constant, until the curves for defluidization from the bubbling state are reached, after which these curves should be followed back to zero gas flow (see line segments EF and ef in figure 8). The observed behaviour is quite different. The bed height initially remains constant only for a very small interval of gas flow, but soon it begins to decrease, following a curve that almost parallels the curve for defluidization from the freely bubbling state. Consequently, when the gas flow reaches zero, the bed height is significantly smaller than the value reached after defluidization from the freely bubbling state. Correspondingly, the pressure drop initially falls for a very short distance, apparently along a line through the origin, but almost immediately it begins to decrease more slowly, following a curve almost parallel to that found in defluidization from the freely bubbling state. Eventually it steepens, as it must, and joins this curve where both come to the origin.

The cycle just described can be followed by a second PC-2 cycle, which starts from the compacted bed reached at zero gas flow in the first cycle. The flow is increased, once more, beyond the point of minimum fluidization, then decreased progressively to zero. The pattern of behaviour is just the same as that observed in the first cycle, but now the height of the compacted bed at the end of the cycle is found to be lower again than that formed at the end of the first cycle (Tsinontides 1992). Indeed, it is possible to run through a whole sequence of cycles, starting with complete defluidization from the freely bubbling state, then following this with a succession of PC-2 cycles, the first two

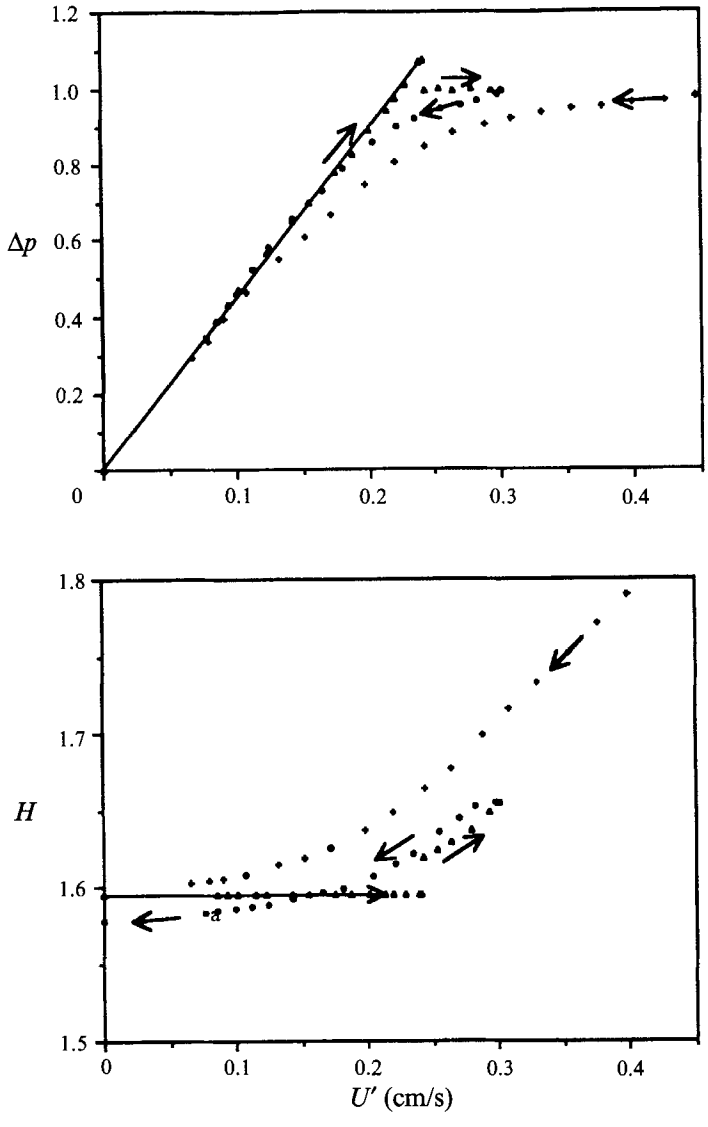


FIGURE 10. PC-2 cycle for cracking catalyst fluidized by wet air in the bed of nominal diameter 2 in.; +, decreasing the gas flow from the freely bubbling state; △, increasing the gas flow from zero; ○, decreasing the gas flow from a partially expanded condition.

of which have just been described. The heights of the completely defluidized beds formed at the ends of the cycles are then found to decrease successively, so the particle assembly is achieving successively tighter packing after each cycle.

Though this observed behaviour in PC-2 cycles differs radically from that predicted by the theoretical arguments presented above, based on the existence of compressive and tensile yield stresses, these simple arguments are unrealistic in that they regard the bed as homogeneous in structure; in particular, the bulk density and the yield stresses are tacitly assumed to be the same everywhere in the bed. This is clearly inappropriate when the particles are not completely supported by the fluid, since the compressive stress within the particle assembly must then increase with increasing depth as a result of the increasing weight of the overburden, and consequently the bulk density would

be expected to increase with increasing depth. It is, therefore, necessary to examine rather more closely the mechanics of expansion and compaction of a particle bed with yield stresses.

## 4. The mechanics of fluidization and defluidization in the presence of yield stresses

For simplicity the presence of lateral bounding walls will be neglected and the bed will be regarded as of infinite extent in the horizontal direction. Then a purely one-dimensional treatment is possible, with stress, bulk density and gas pressure depending only on a co-ordinate $x'$, measured vertically downward from the surface of the bed. Furthermore, only the $xx$-component of the stress tensor of the particle phase is relevant, and this will be denoted by $\sigma'$, defined in the compressive sense. Then for a bed at rest a force balance on the particulate material gives

$$\frac{\mathrm{d}\sigma'}{\mathrm{d}x'} = \rho_p(1-\epsilon)g - \beta(\epsilon)u', \tag{5}$$

where $\rho_p$ denotes the density of the solid material from which the particles are formed, $\epsilon$ is the local void fraction of the particle assembly, $g$ is the gravitational acceleration and, in the last term on the right-hand side which represents the drag force per unit total volume exerted on the particles by the gas, $u'$ is the interstitial average gas velocity. For particles in this size range it is reasonable to adopt the well-known expression of Richardson & Zaki (1954) for $\beta(\epsilon)$, namely

$$\beta(\epsilon) = \frac{\rho_p(1-\epsilon)g}{v_t}\frac{1}{\epsilon^{n-1}}, \tag{6}$$

where $v_t$ is the terminal velocity of fall of an isolated particle in the gas, and the exponent $n$ depends on the Reynolds number for a particle falling with this velocity. Adding (5) above to a corresponding force balance for the gas gives an overall force balance in the form

$$\frac{\mathrm{d}p'}{\mathrm{d}x'} + \frac{\mathrm{d}\sigma'}{\mathrm{d}x'} = \rho_p(1-\epsilon)g. \tag{7}$$

We must also impose the conditions that $\sigma' = 0$ at the free surface $x' = 0$, and that the total mass of material is fixed, so that

$$\rho_p \int_0^{H'} (1-\epsilon)\,\mathrm{d}x' = m, \tag{8}$$

where $H'$ is the depth of the bed and $m$ is the mass of solid material loaded, per unit cross-sectional area. It is convenient to introduce dimensionless variables defined as follows:

$$\sigma = \sigma'/mg, \quad p = p'/mg, \quad x = x'\rho_p/m, \quad H = H'\rho_p/m, \quad u = u'/v_t.$$

Then, after introducing $U = \epsilon u$, combining (5) and (6), and integrating (7) over the depth of the bed, we find

$$\frac{\mathrm{d}\sigma}{\mathrm{d}x} = (1-\epsilon)\left[1 - \frac{U}{\epsilon^n}\right], \tag{9}$$

$$\sigma(H) + \Delta p = 1, \tag{10}$$

$$\int_0^H (1-\epsilon)\,\mathrm{d}x = 1, \tag{11}$$

where $\Delta p = p(H) - p(0)$, the overall dimensionless gas pressure drop across the bed.

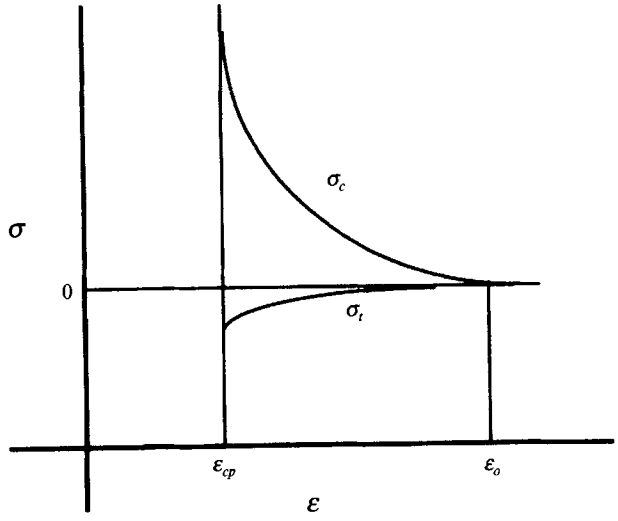


FIGURE 11. Sketch of the anticipated dependence of compressive and tensile yield stresses of the particle assembly on void fraction.

We now assume that the assembly of particles is capable of resisting compression when its bulk density exceeds some minimum value, corresponding to a void fraction $\epsilon_o$. We also assume that the stress needed to cause compressive yield increases as $\epsilon$ decreases below $\epsilon_o$, and tends to infinity at some smaller value $\epsilon_{cp}$ of the void fraction. (In practice the individual particles would begin to fracture at some large, but finite value of the stress.) For large, smooth, identical particles, such as ball bearings or glass beads, a void fraction close to random close packing is achieved under the smallest compacting force, and this void fraction does not change much as the applied force is increased. Thus $\epsilon_o$ and $\epsilon_{cp}$ are very close together. However, when cohesive forces between particles in contact are significant, or the particle surfaces are rough, so that there is significant resistance to sliding at their points of mutual contact, the assembly of particles does not collapse to close packing so easily, and more extended structures can be formed which are still capable of resisting compressive forces. Correspondingly the gap between $\epsilon_{cp}$ and $\epsilon_o$ is much larger for particles of this type. Cracking catalyst is a material belonging to Group A of Geldart's (1973) classification, and cohesive forces between particles in contact might be expected to be of a similar order as the weight of a particle. Also, the surface of the micro-porous silica–alumina particles would be expected to have a friction coefficient larger than that of polished glass or steel. Thus, for this material, we should expect a compressive yield stress to exist over a wide interval of void fraction. The cohesive forces will also ensure that the material can sustain some non-vanishing tensile stress before dilating irreversibly; in other words, there will be a tensile yield stress, whose magnitude would be expected to increase with increasing bulk density. It follows that the yield stresses of the particle assembly, for one-dimensional yielding, would be expected to have the form sketched in figure 11, which shows the compressive yield stress $\sigma_c$ and the tensile yield stress $\sigma_t$, as functions of the void fraction. When the stress varies between these limits the bed will behave elastically, and we expect very little change in void fraction with stress within this interval.

Returning now to (9), when $\sigma$ lies between the yield limits this equation determines

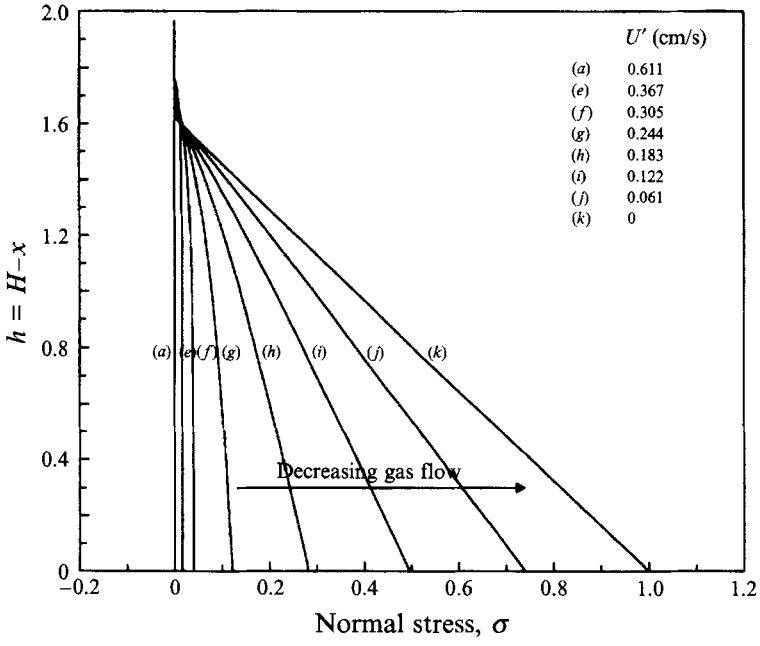


FIGURE 12. Computed variation of dimensionless normal stress with height, presented for successively decreasing values of the gas flow.

how it will depend on $x$. When the bed is in compressive yield, on the other hand, $\sigma = \sigma_c(\epsilon)$, and (9) determines how the void fraction depends on $x$. Similarly, if the bed is in tensile yield, $\sigma = \sigma_t(\epsilon)$, and (9) again determines the dependence of void fraction on depth. Once the void fraction and stress profiles are known, (10) determines the overall gas pressure drop, and (11) the total height of the bed.

Let us first consider progressive defluidization of the bed from an initial void fraction larger than $\epsilon_o$. We shall assume that the bed is in compressive yield everywhere during the process of compaction as the gas flow is decreased, so (9)–(11) are to be solved with $\sigma_c(\epsilon)$ substituted for $\sigma$. For this purpose an explicit expression for $\sigma_c$ is assumed, of the form

$$\sigma_c = C\frac{(\epsilon_o - \epsilon)^a}{(\epsilon - \epsilon_{cp})^b} \quad \text{for} \quad \epsilon \leqslant \epsilon_o$$
$$= 0 \qquad\qquad\quad \text{for} \quad \epsilon > \epsilon_o, \tag{12}$$

where $C$, $a$ and $b$ are constants. Equations (9)–(11) are then solved numerically, and the resulting profiles of dimensionless stress and solids fraction $(1-\epsilon)$ are shown, at various stages of defluidization down to zero gas flow, in figures 12 and 13. The results exhibited correspond to the following parameter values: $m = 35.7$ g/cm$^2$, $n = 4.0$, $C = 1.25 \times 10^{-3}$, $a = 1$, $b = 2$, $\epsilon_o = 0.49$, $\epsilon_{cp} = 0.363$, $v_t = 10.6$ cm/s. These values for $m$, $v_t$, $\epsilon_o$ and $\epsilon_{cp}$ match those of the experimental system.

At each value of the gas flow figure 13 shows that the bulk density builds up with increasing depth, as expected, with most of the increase occurring quite close to the surface. The height of the bed decreases and the bulk density increases as the gas flow decreases, and curve ($k$) shows the density profile of the gravitationally compacted bed, with no gas flow. The stress would build up linearly with depth in a bed of uniform density, and the deviations from linearity in the plots of figure 12 simply reflect the

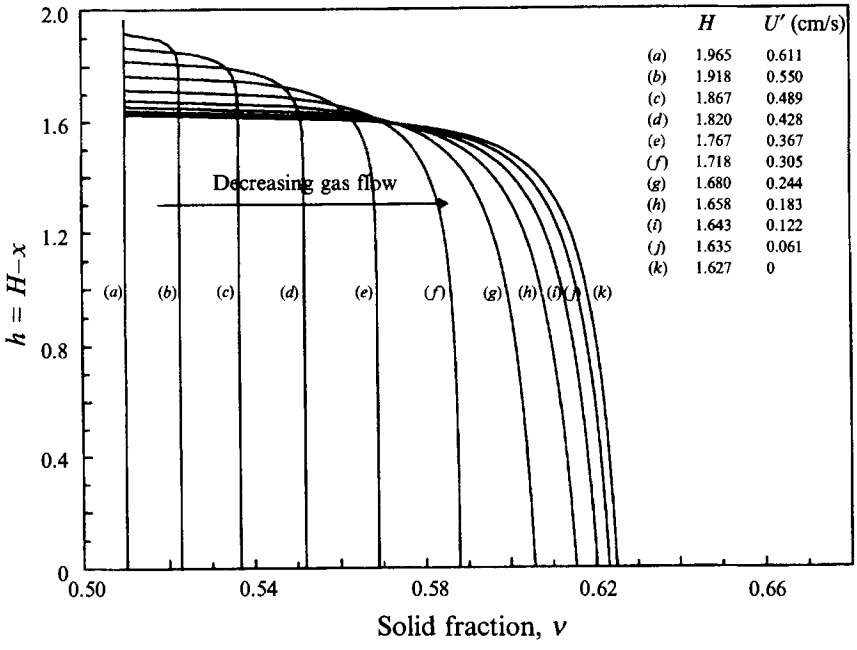


FIGURE 13. Computed variation of solids fraction with height, presented for successively decreasing values of the gas flow.

density profiles of figure 13. The computed variations in dimensionless pressure drop and bed height with gas flow are shown in figure 14, and these are seen to have just the shape of the experimental observations recorded in figures 5–8, with no breaks at the condition of minimum fluidization.

If the gas flow is now progressively increased by small increments from zero, the stress profiles initially lie entirely between the yield limits, and they are generated by integrating (9) with $\epsilon(x)$ found from the curve (*k*) of figure 13. A sequence of these profiles, for successively larger values of the flow, is shown in figure 15. The tensile yield stress of the bed (figure 11) is an increasing function of the bulk density so, bearing in mind the density profile, it must vary down the bed in the way indicated by the broken curve in figure 15. There is also a tensile yield stress between the lowest layer of particles in the bed and the surface of the distributor, and this might be expected to be of the same order of magnitude as the yield stress within the bed at this point. Then it is clear from figure 15 that, as the gas flow is increased progressively, the condition for tensile yield will be met first either at the contact between the bed and the distributor, or within the bed at its lowest point, but not at any higher level. Thus, for this type of material, fluidization must be initiated by fracture of the bed at its lowest point. The necessary value of the gas pressure drop is the sum of the weight of the bed and the tensile yield stress which must be broken, so this yield stress is measured by the observed overshoot of the pressure drop curve beyond the bed weight at minimum fluidization.

Once the adhesion at the base of the bed is broken the lower boundary becomes a free surface, with zero stress, so the stress vanishes at both the upper and lower surfaces, while taking positive (i.e. compressive) values in between. Then since the drag force on the bed at rest exceeds its weight, the bed as a whole accelerates upward without any deformation until the relative velocity of particles and gas is reduced to the point where the drag force just balances the weight. The bed could then, in principle,

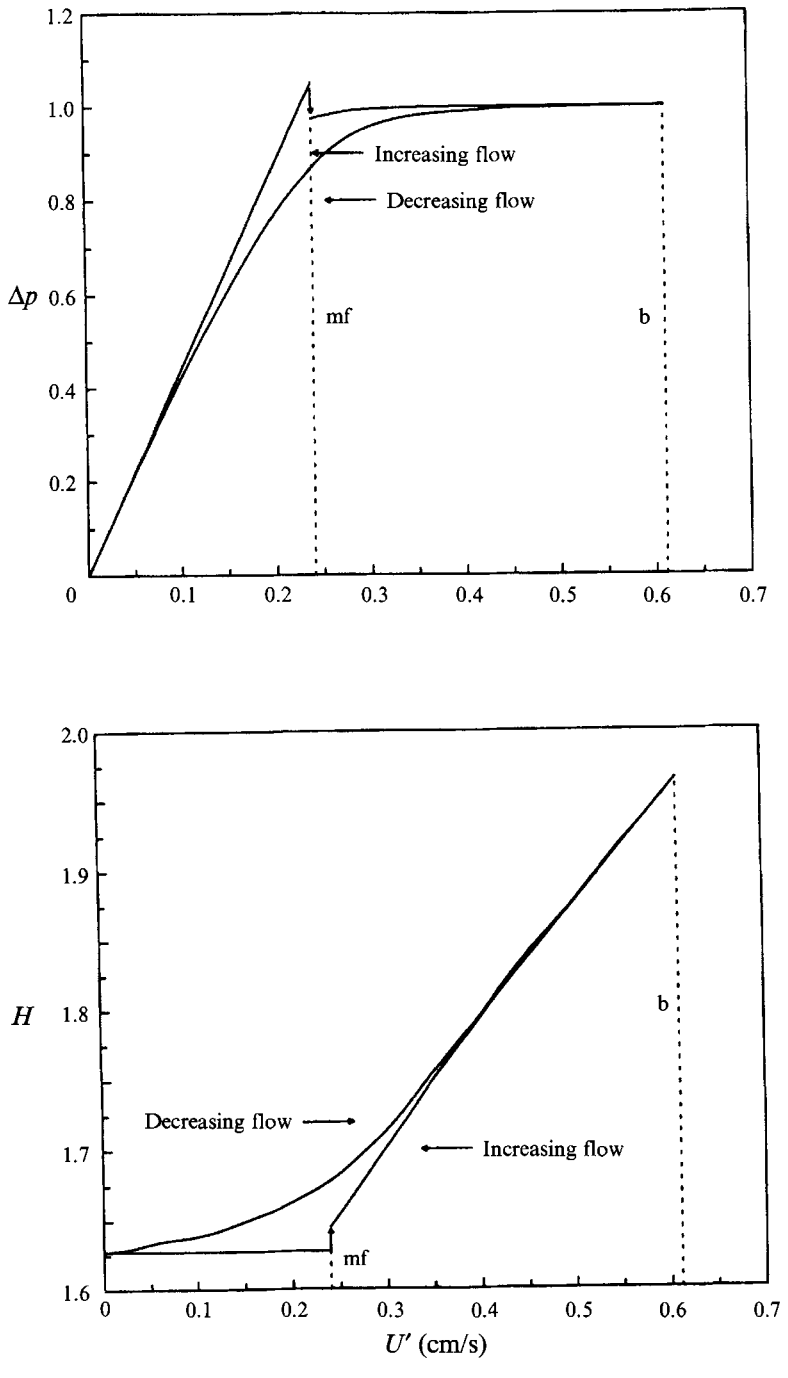


FIGURE 14. Computed curves showing dimensionless pressure drop and dimensionless bed height, as functions of the gas superficial velocity, for a complete fluidization–defluidization cycle.

continue to move upward indefinitely as a plug at this speed, but in practice the exposed lower surface is unstable and will erode, generating a rain of particles behind it. These then sediment through the air stream and eventually recompact to form a new bed which is at rest and in force balance with the gas flow. The upper section of the

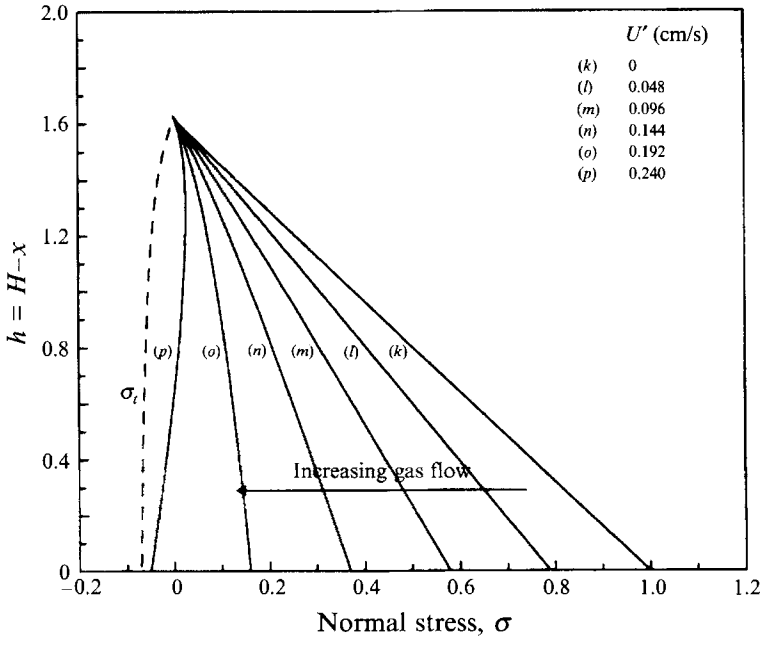


FIGURE 15. Computed variation of normal stress with height, presented for the fully compacted bed at successively increasing values of the gas flow, each less than the flow corresponding to minimum fluidization.

original packed bed continues to move upward under the influence of the drag force exerted by the gas but, as it erodes to progressively shorter length, the mean bulk density becomes smaller, since it represents that part of the original bed adjacent to the upper surface. Thus, the moving plug must slow down as it rises to maintain a balance between its weight and the drag force exerted on it by the gas. If the gas flow is not much larger than that corresponding to minimum fluidization, the plug will come to rest before its length shrinks to zero. The new, expanded bed will then consist of this remnant of the upper section of the original packed bed, present before the point of minimum fluidization, at rest above a new bed formed by sedimentation of the particles which were shed from its unstable lower surface as it rose.

This picture of the process of bed expansion in a cohesive material of this type is very different from the conventional idea of fluidization, as a uniform dilation occurring throughout the assembly of particles. Dilation is confined to a narrow 'shock' region at the eroding lower surface of the undeformed upper section of the original bed, and the rest of the process contributing to the formation of the new, expanded bed is a recompaction. The zone of dilation can actually be followed visually as it moves up through the bed after a small increment of gas flow above minimum fluidization, and it can be seen to come to rest before it reaches the upper surface of the bed, as predicted by the argument above. Lacking an exact understanding of the mechanics of erosion of the unstable lower surface of the rising plug, quantitative modelling of the bed at successive stages of expansion involves some arbitrary assumptions. For example, if we assume that there is no discontinuity in bulk density at the bottom of the upper undisturbed plug, and that the bed below is entirely supported by the drag force, and of uniform bulk density, then the profiles of stress and volume fraction solids shown in figures 16 and 17 are obtained. The profiles labelled ($p$) correspond to a gas flow just

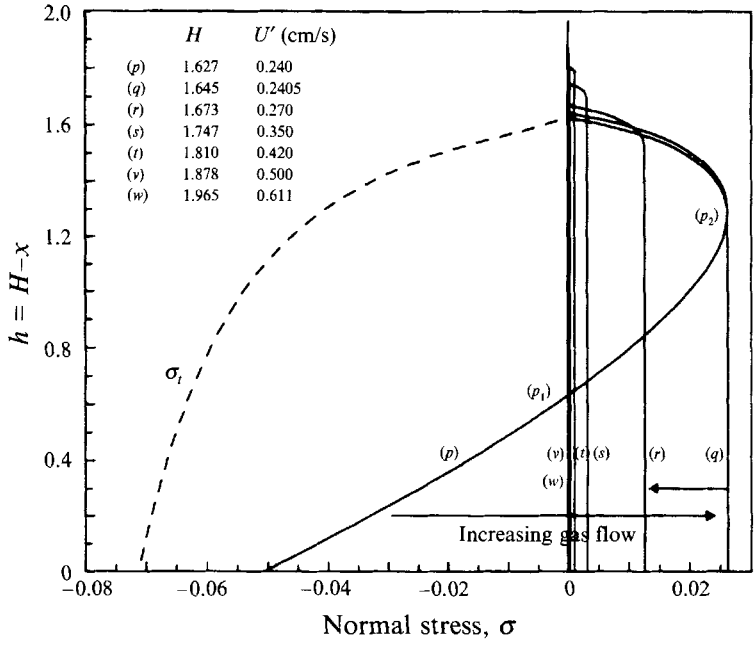


FIGURE 16. Computed variation of normal stress with height, presented for an increasing sequence of values of the gas flow, starting just below the value corresponding to minimum fluidization.

below minimum fluidization, then profiles (*q*)–(*w*) show how the situation develops with successive increases in gas flow. These results allow figure 14 to be completed, and it is seen that most major features of the observations recorded in figures 5–8 are reproduced. There is even the small dip in the pressure drop, below the bed weight, immediately following minimum fluidization, followed by a rise to a value quite close to the bed weight. Only the observed dip in the curves for increasing flow rate, observed just before they join the curves for decreasing flow rate, is missing from the predicted behaviour.

The above treatment can be extended to the cases of PC-1 and PC-2 partial cycles, of the sort investigated experimentally. The PC-1 cycle starts from a partially compacted bed; that is, from one of the states shown in detail in figures 12 and 13 and, as the gas flow is increased, the stress everywhere in the bed at first lies between the yield limits, so the bed does not deform and the pressure drop is proportional to the flow rate. As in a complete cycle, tensile yield is initiated at the bottom of the bed, but less tensile stress is needed than was the case when starting from zero gas flow. The picture is, therefore, essentially the same as the curve for increasing gas flow in a full cycle, and it accords fully with the observations recorded in figure 9.

The predicted behaviour in a PC-2 cycle depends on the bulk density profile in the partially expanded bed from which it starts and, as we have seen, there is some uncertainty about this, stemming from the nature of the dilation across a 'shock'. However, accepting the profiles presented in figures 16 and 17, the progress of compaction with decreasing gas flow during a PC-2 cycle can be predicted by the methods already described. Details are given by Tsinontides (1992), who shows that compaction begins at the bottom of the bed, while the upper part initially descends as a plug. As the gas flow decreases, the compacting region spreads upward until the whole bed is in compressive failure when the gas flow falls to zero. The predicted

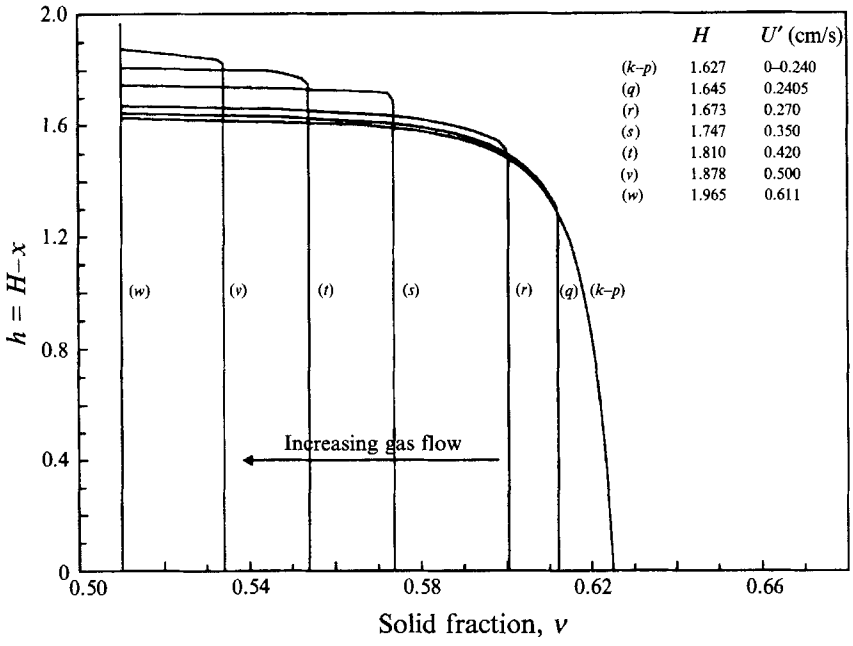


FIGURE 17. Computed variation of solids fraction with height, presented for an increasing sequence of values of the gas flow, starting just below the value corresponding to minimum fluidization.

behaviour of the pressure drop and bed height during this process is shown, for two different cycles, in figure 18. Comparing this with figure 10, it is seen that some features of the observed cycles are reproduced qualitatively. Thus, the bed height begins to decrease with decreasing gas flow after remaining almost constant for some time and, correspondingly, the pressure drop deviates from a straight line through the origin. However, the effects are not nearly so marked as those observed experimentally. In particular, the bed height at zero gas flow is predicted to be the same as that attained after progressive defluidization from a freely bubbling bed, whereas a very striking result of the observations was the fact that the bed height at the end of a PC-2 cycle is significantly smaller than that attained in defluidization of a bubbling bed. We shall return to this discrepancy later.

Equation (10) relates the stress $\sigma(H)$ at the bottom of the bed to $\Delta p$, and (11) relates the mean void fraction of the bed to $H$. Thus, if our neglect of wall friction were justified, from a complete fluidization–defluidization cycle, together with a set of PC-1 partial cycles giving results such as those plotted in figure 9, it would be possible to relate both the compressive yield stress and the tensile yield stress to the mean void fraction. The values of $\Delta p$ at the overshoot peaks of the PC-1 cycles would give $\sigma_t$, the tensile stress at which the bottom of the bed and the distributor part company when the gas flow is increased. On the other hand, the values of $\Delta p$ from the curve representing compaction from the freely bubbling bed would give $\sigma_c$, the compressive yield stress for the material in contact with the distributor, and the bed height measurements would give the mean void fraction for the bed as whole. Though neglect of wall friction certainly cannot be justified in interpreting our experiments quantitatively, it is nevertheless interesting to plot 'pseudo' yield stresses, deduced from our measurements in the way just described, against the mean void fraction. Figure 19 shows these for a bed fluidized by moist air in the nominal 2 in. diameter

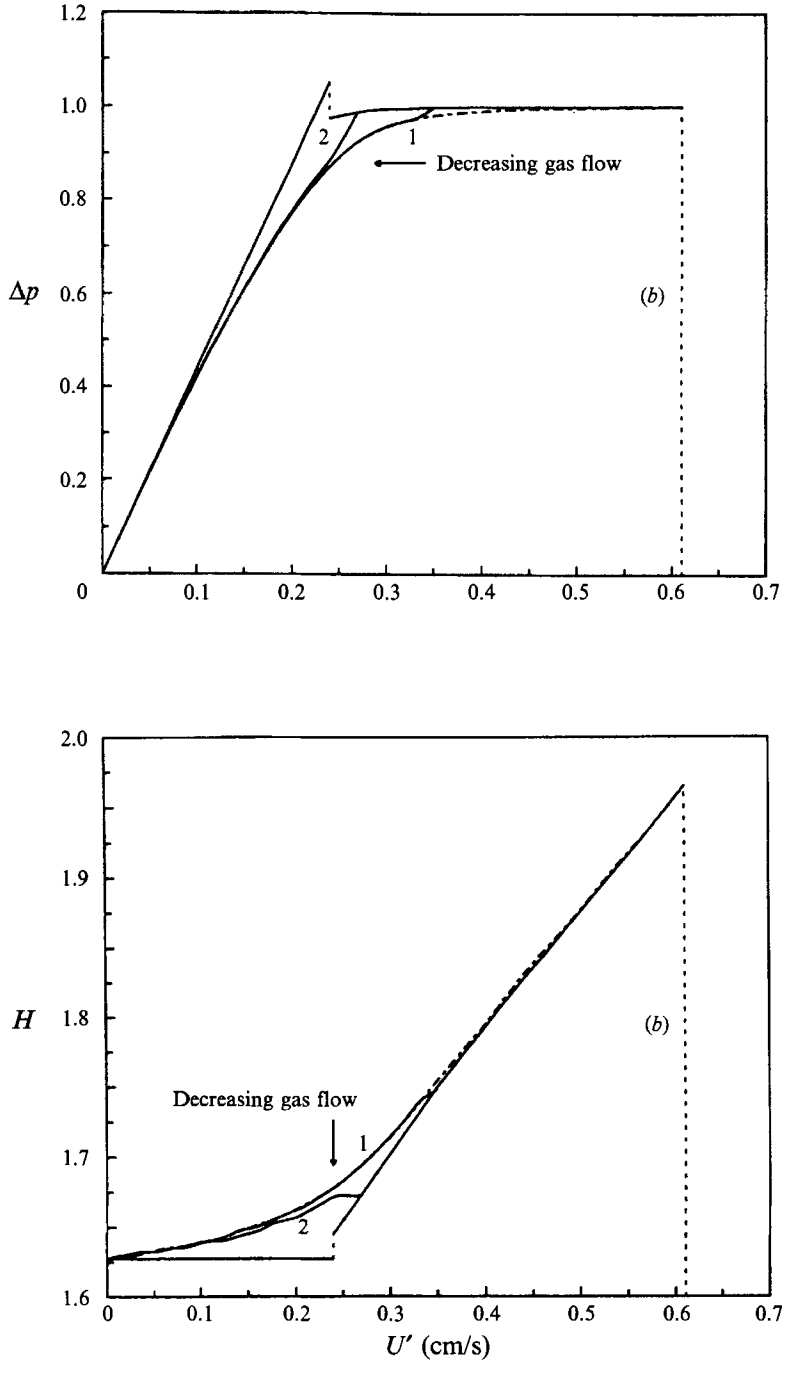


FIGURE 18. Computed curves showing dimensionless pressure drop and dimensionless bed height, as functions of the gas superficial velocity, for two different PC-2 cycles.

tube. In principle the effects of wall friction could be 'filtered' out of the results by repeating the programme of measurements for beds of several different depths and diameters, and comparing the results with predictions of a modified theory which takes into account wall friction, possibly by an approximate procedure of the well-known

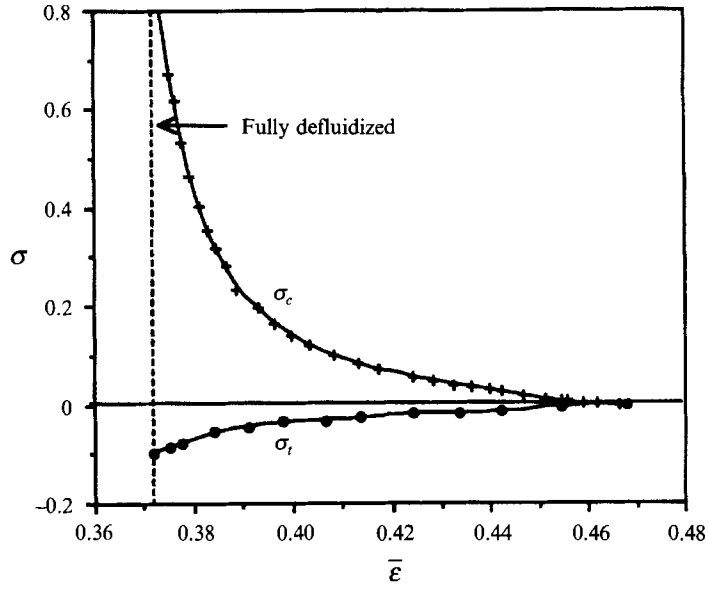


FIGURE 19. Values of the dimensionless tensile and compressive 'pseudo' yield stresses inferred from the experiments with neglect of wall friction, plotted against the mean void fraction of the bed.

Janssen (1895) type. Indeed, it is even tempting to draw conclusions about wall friction by simple arguments applied to certain specific differences between our measurements in 1 in. and 2 in. diameter tubes; for example, the overshoots of the pressure drop beyond the bed weight at the point of initial expansion. The observed overshoot may be a result of tensile yield stress (the only possibility in the absence of bounding walls), a result of friction between the particulate material and the bounding walls, or some combination of the two, and the contributions to overshoot from these two causes should depend on the diameter and depth of the bed in different ways. Unfortunately, the presence of an extended region below the upper surface of the bed, over which the void fraction varies significantly, invalidates simple arguments about the form of these dependences. To discriminate unambiguously between the two causes of overshoot the observations must be compared with predictions from a theory extended to take wall friction into account. We intend to extend the theory in this way and conduct further experiments of the sort described here, over a range of bed heights and diameters.

The curious behaviour of the bed during compaction in a PC-2 cycle, noted above and recorded in figure 10, remains a puzzle and suggests that the structure of the expanded bed between minimum fluidization and minimum bubbling may be more complicated than we have assumed. To probe this question further, and to check other predictions of the simple theory, measurements of density profiles during fluidization and defluidization were undertaken.

## 5. Measured bulk density profiles during progressive fluidization and defluidization

Most of the density profiles were determined in a bed of 450.1 g of catalyst, loaded in the 2 in. nominal diameter tube and fluidized with dry air. A smaller number of measurements was made with periodic injections of small amounts of ammonia vapour in the fluidizing air (a common device used to alleviate the effects of static electricity

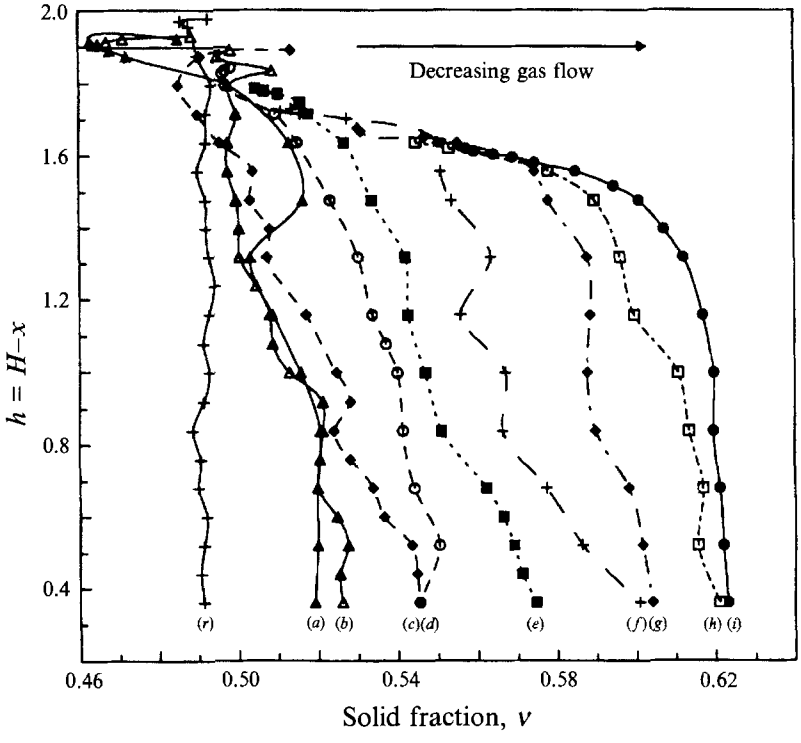


FIGURE 20. Experimentally determined profiles of solids fraction as a function of height, along the centreline of a bed of 450.1 g of cracking catalyst fluidized by dry air in the bed of nominal diameter 2 in. Profiles are presented for a decreasing sequence of values of the gas flow, starting from a freely bubbling bed (*r*) and ending at zero flow (*i*).

in experiments with cracking catalyst) and with the dry air replaced by moist air, to make sure that the phenomena we observed were not peculiar to the catalyst–dry air combination. Though the measurements give the bulk density directly, they are presented as volume fraction of solids, obtained by dividing the measured bulk density by a particle density assumed to be 1.44 g/cm$^3$. Since the particles are micro-porous there is some uncertainty in this value, but there is an advantage in scaling the bulk density in this way to give an impression of the extent to which the particles fill space. Nevertheless, it should be borne in mind that the bulk density, rather than the volume fraction, is the figure to which absolute significance may be attached.

Figure 20 shows a set of profiles along the axis of the bed for successive stages of defluidization, starting from a freely bubbling bed, the relevant profile for which is labelled (*r*). As the flow of gas is reduced progressively the sequence of profiles labelled (*a*)–(*i*) is obtained, where profile (*i*) corresponds to the completely defluidized bed with no gas flow. Figure 21 identifies, on a plot of $\Delta p$ versus $U'$, the conditions for which the profiles were measured. Recall that each point on a profile represents an average bulk density over a period of 15–20 min, for which counts were accumulated by the detector. Questions of precision and spatial resolution have been discussed above. They can usefully be summarized by saying that the experimental uncertainties, in both the horizontal and vertical directions on the plots, are of the order of twice the size of the icons used to identify the measured points.

For the bubbling bed there is very little variation in the time-average bulk density with depth, but as soon as the gas flow is reduced slightly below the bubbling point

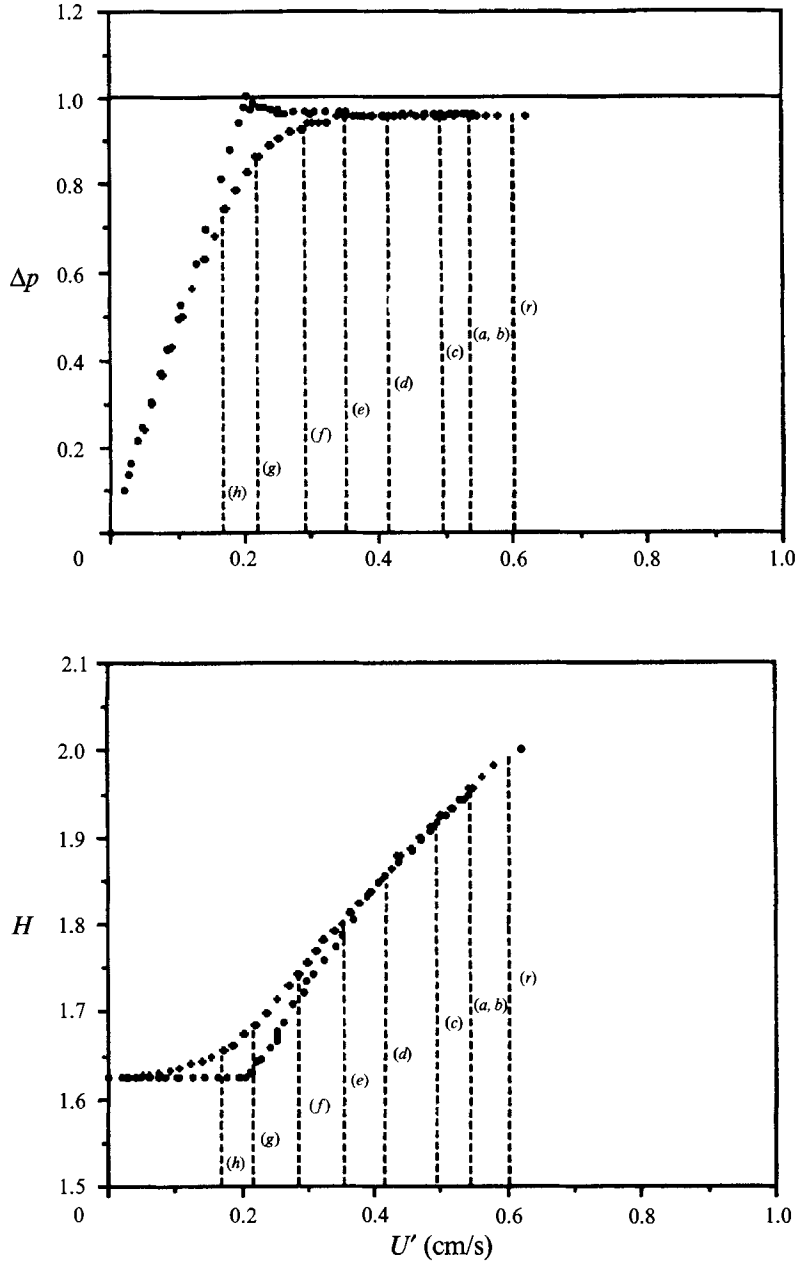


FIGURE 21. Identification of the gas flows corresponding to the profiles shown in figure 20, in relation to the fluidization–defluidization cycle.

there is a significant increase of density with depth, as seen from profiles (*a*) and (*b*). These were measured one after the other, without changing the gas flow, and although they are generally similar, there are significant differences of detail. For lower values of the gas flow, on the other hand, the profiles were found to be reproducible in detail if the gas flow was not altered, even after periods of several hours. Clearly the transmitted stresses are so small, under the conditions of profiles (*a*) and (*b*), that the bed has hardly any mechanical strength, and the smallest mechanical disturbances

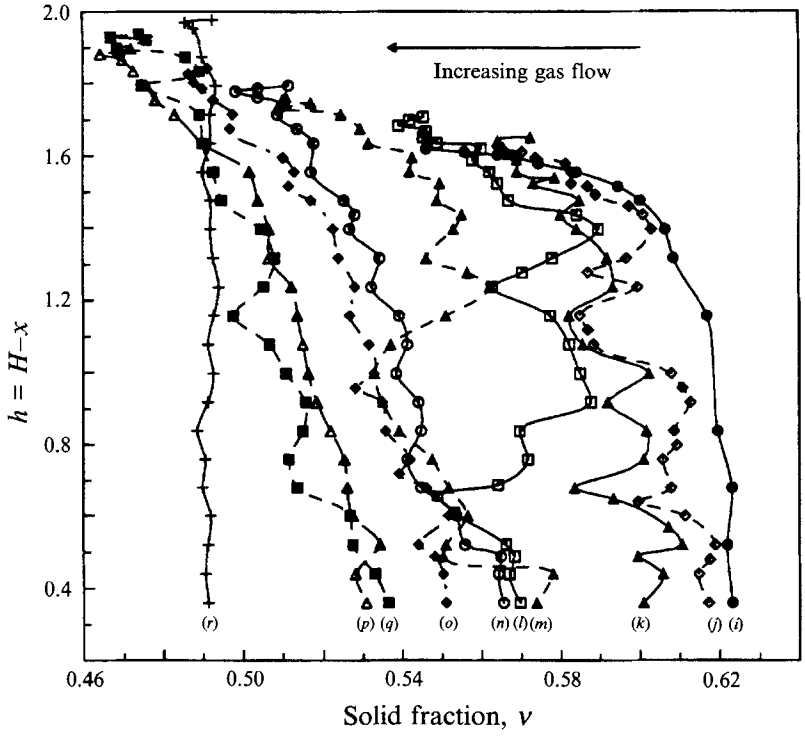


FIGURE 22. Experimentally determined profiles of solids fraction as a function of height, along the centreline of a bed of 450.1 g of cracking catalyst fluidized by dry air in the bed of nominal diameter 2 in. Profiles are presented for an increasing sequence of values of the gas flow, starting from zero and ending at a value corresponding to a freely bubbling bed.

(rarely specifically identifiable) can change the profile, whereas at lower flows the structure formed is quite robust. The measured sequence of profiles closely resembles that predicted theoretically and recorded in figure 13. There are some irregularities in the measured densities, but over most of the depth the deviations from a smooth curve are within the bounds of experimental uncertainly. An exception to this statement must be made for the measured points closest to the free upper surface of the bed, but here the transmitted stress is always small, so the structure of the particle assembly is weak and subject to disturbance during even the most careful movements of the bed. Consequently we are not confident that they should be interpreted as indicating any important mechanical features of the bed. Profile (*i*), for the fully defluidized bed, shows the density to be essentially constant over much of the depth, with a substantial drop off near the upper surface.

Figure 22 shows a sequence of density profiles for the process of refluidization, as the gas flow is increased progressively from zero to the value, corresponding to a bubbling bed, from which figure 20 started. Figure 23 identifies the corresponding points on the $\Delta p$ versus $U'$ plot. Before the point of minimum fluidization profile (*i*) remains completely unchanged. Profile (*j*) corresponds to a gas flow just above the point of minimum fluidization, then the remaining profiles were taken after successive increments in flow. All the profiles were robust, in the sense that the measurements could be reproduced in detail after a lapse of several hours, except for the penultimate one (profile *q*), which was taken very near to the bubbling point. These profiles exhibit a new, and quite unexpected feature, namely quasi-periodic spatial variations in the

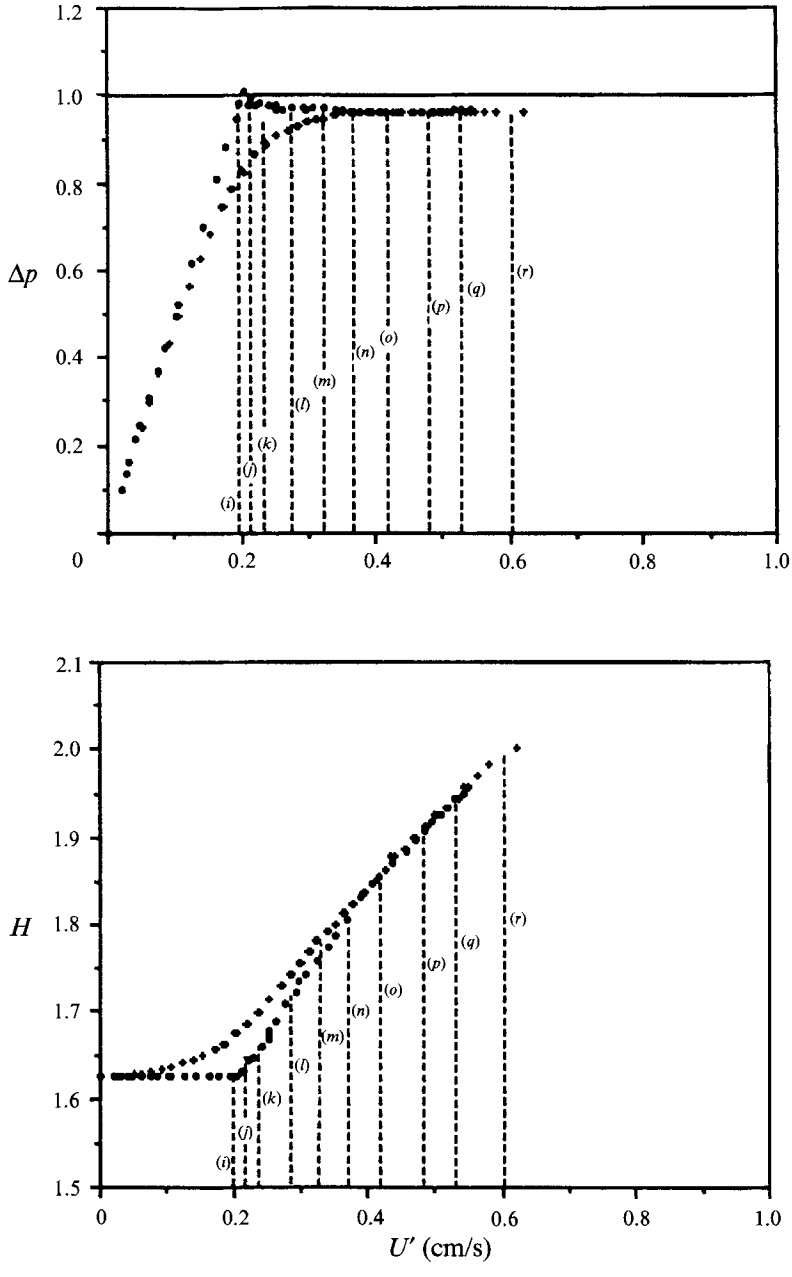


FIGURE 23. Identification of the gas flows corresponding to the profiles shown in figure 22, in relation to the fluidization–defluidization cycle.

time-average density with height. The wavelength of these variations is a few centimetres and their amplitude is well outside the bounds of experimental error; indeed, in the middle of the interval of flow separating minimum fluidization from minimum bubbling (profiles *l* and *m*) they are quite large. If the process of fluidization is restarted from zero gas flow, statistically similar variations in density to those shown in figure 22 are observed at corresponding values of the gas flow, though the profiles are not reproduced in detail.

These results suggest that the bed consists of alternating horizontal layers of high and low density, though similar axial density profiles could conceivably result from the presence of a narrow, tortuous channel of low density (or 'rathole') that zigzags back and forth across the centreline. Separate bulk density scans across the bed in fixed horizontal planes (Tsinontides 1992) revealed no evidence of the presence of such ratholes, so it can be concluded that the observed density variations are essentially one-dimensional, depending only on the vertical coordinate. The presence of structures of this kind, which are able to survive unchanged over long period of time (at least from day to day if the apparatus is not grossly disturbed) is quite inconsistent with any picture of a bed stabilized by one of the proposed hydrodynamic mechanisms (Foscolo & Gibilaro 1984; Batchelor 1988). We speculate that the observed structures have their origin in the detailed mechanism of bed expansion, described above, for a cohesive material. After an increase in gas flow the new, more expanded bed is actually formed by compaction from a sedimenting suspension of particles shed from the lower surface of a rising plug. In this suspension interparticle forces would be expected to be small, so a uniform distribution of particles will be unstable (Jackson 1963). The instability will take the form of density waves propagated upward through the assembly of particles. These will survive until the increase in bulk density leads to a significant yield stress, at which point they will no longer be able to propagate, and the waveform will become 'frozen' in the compacted bed. This frozen waveform is what we observe in the density profiles.

The presence of the density striations immediately suggests the reason for the anomalous behaviour observed when the gas flow is reduced, with such a state as the starting point, as in a PC-2 cycle. As the part of the weight of the particles borne by the drag force decreases, the assembly of particles would be expected to yield first (in compression) at those places where it is weakest, namely the planes of lowest bulk density. Thus the process of compaction should start here then spread progressively to the denser parts of the bed as the gas flow is reduced, in contrast to our theoretical treatment, which is based on an assumption that the whole bed is in compressive yield. If this hypothesis is correct, it should be possible to observe the selective increase in density in the weakest places by measuring density profiles as the gas flow is reduced progressively in a PC-2 cycle. Figure 24 shows the results of such an experiment. Curve (*a*), which is the density profile of a fully compacted bed formed by progressive reductions in gas flow, starting from a freely bubbling state, shows a monotone increase in density with depth, with some superimposed local fluctuations which may or may not be real as their magnitude is close to the limit of experimental precision. If the gas superficial velocity is then increased progressively to 0.271 cm/s, above the point of minimum fluidization, the density profile labelled (*b*) is measured, showing the typical quasi-periodicity of beds in the 'interval of uniform fluidization' between minimum fluidization and minimum bubbling. For very small reductions in gas flow, starting from this superficial velocity, the density profile remains unchanged, but when the superficial velocity has been reduced to 0.229 cm/s the density profile labelled (*c*) is measured. Comparing this with profile (*b*) it is seen that there has been substantial compaction of the regions of lowest density, and a much smaller compaction of the denser regions, with the result that the amplitude of density variations is much smaller in profile (*c*) than in profile (*b*). This confirms our speculation above about the mechanism of compaction. A further reduction in gas flow, to a superficial velocity of 0.195 cm/s, leads to profile (*d*) and, finally, when the flow is reduced to zero the density profile labelled (*e*) is obtained. The bulk density is then everywhere larger than in the initial profile (*a*) and, correspondingly, the total height of the bed is smaller. Thus, we

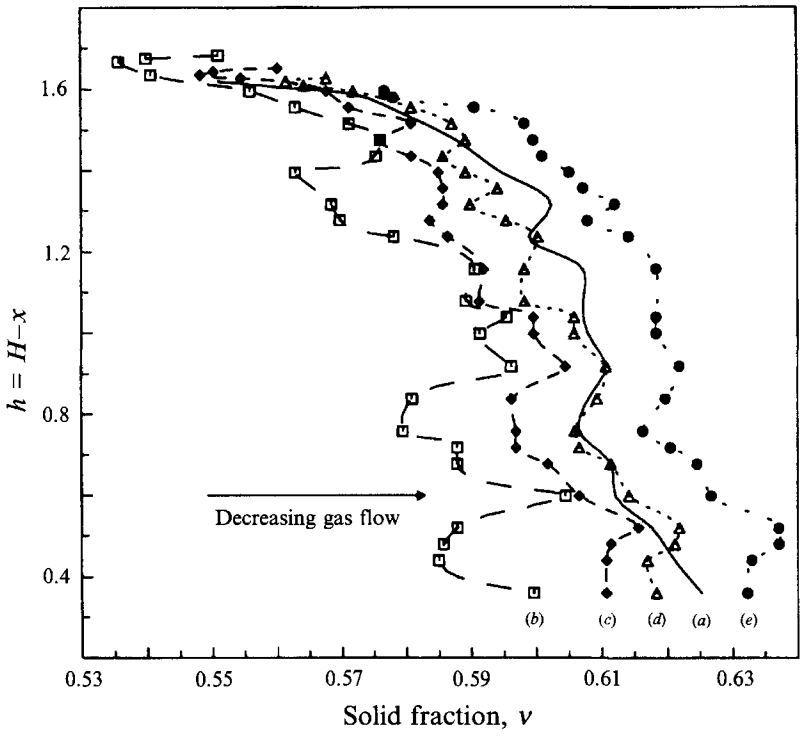


FIGURE 24. Experimentally determined profiles of solids fraction as a function of height, along the centreline of a bed of 450.1 g of cracking catalyst fluidized by dry air in the bed of nominal diameter 2 in. Profiles are presented for a decreasing sequence of values of the gas flow, starting from a value larger than that corresponding to minimum fluidization, but smaller than that required for free bubbling.

have been able to follow in detail the puzzling process of compaction during a PC-2 cycle, and can see how the final bulk density becomes larger than that of a bed formed by defluidization from the freely bubbling state.

## 6. Summary and conclusions

Though publications by Rietema and co-workers, cited earlier, provide compelling evidence for the existence of particle–particle contact forced in 'fluidized' beds of fine particles and, if large enough, their link to the question of stability is clear, we believe the additional evidence provided by the present investigation of cracking catalyst confirms unequivocally that the extended interval of stable expansion which is observed to separate 'minimum fluidization' and 'minimum bubbling' in this system is, indeed, a consequence of contact forces between the particles. A limited number of experiments on fine sand, of 154 μm mean diameter, show that this too exhibits a hysteresis indicative of the presence of yield stresses, though much less pronounced than the hysteresis observed with cracking catalyst. Figure 25 shows pressure drop and bed height curves for a full defluidization–fluidization cycle for 200 g of the sand, fluidized with dry air in the 1 in. nominal diameter tube. The hysteresis between the curves for increasing and decreasing gas flows is narrow, but clearly visible and, most significantly, there is a short interval of stable behaviour between minimum fluidization and minimum bubbling, whose terminus coincides with the point at which the hysteresis loop closes, indicating the vanishing of yield stresses. Thus, here again, the

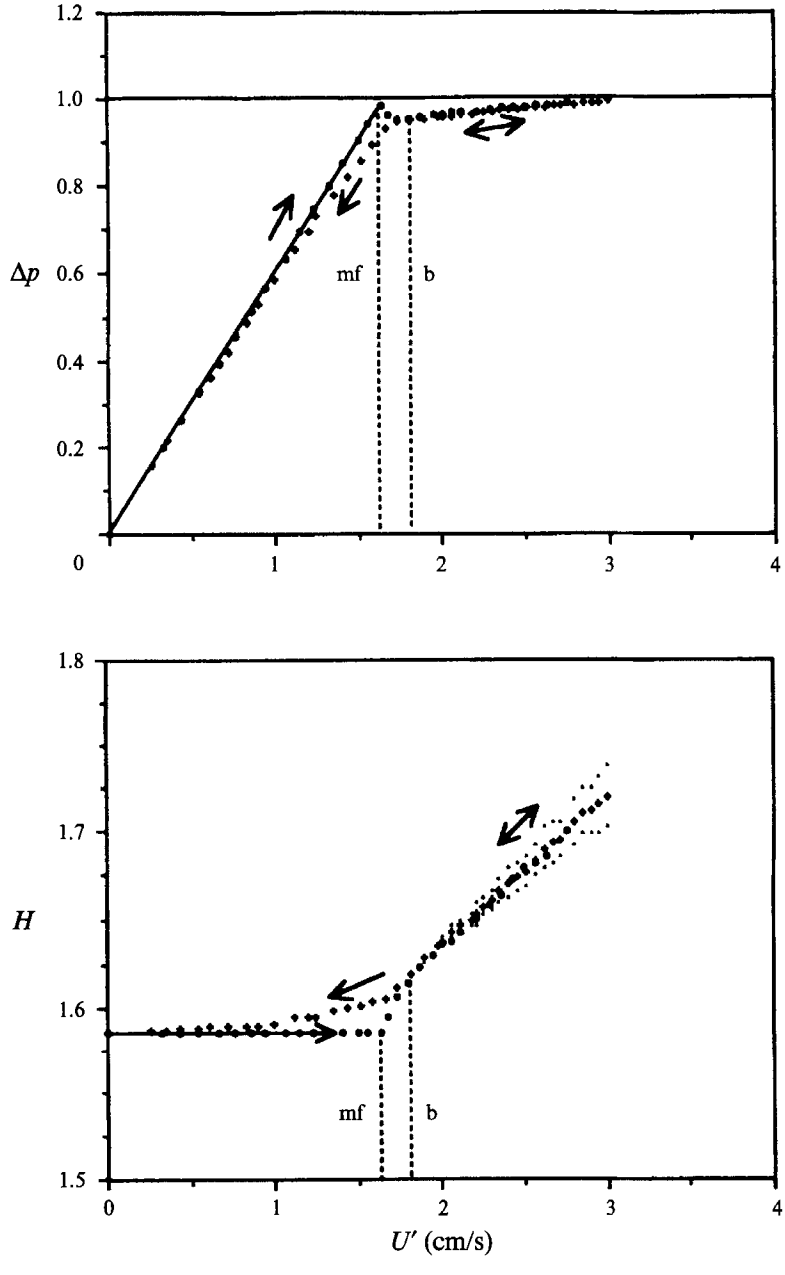


FIGURE 25. Dimensionless pressure drop and bed height, as functions of the gas superficial velocity, for sand fluidized by dry air in the bed of nominal diameter 1 in.; ●, increasing gas flow; +, decreasing flow.

mechanism of stabilization appears to be yield stresses resulting from solid–solid contacts.

It has been argued that contact forces cannot be responsible for stabilization in fluidized beds since, if they were, the point of minimum bubbling would surely depend on factors such as humidity and electrostatics, which must influence the magnitude of the contact forces. The implication here is that no such dependence of the minimum

bubbling condition is observed in practice. In attempting to address this contention we must take into account that changes in the experimental conditions expected to change the magnitude of the contact forces usually have a secondary effect of changing other properties, which also influence the minimum bubbling point. For example, the change from dry to moist air changes the density and viscosity of the fluidizing gas, and also the density of the catalyst particles themselves, as a result of adsorbed water. Thus, though comparison of figures 5 and 7, or figures 6 and 8, for fluidization with dry and moist air respectively, reveals significant differences in both the gas velocity and the bed expansion at minimum bubbling, it is not clear how much of this should be attributed to modification of surface forces and how much to these other factors. However, it is easy to eliminate the difference in physical properties between dry and moist air as the cause of the observed difference in behaviour. Instead of using catalyst which has been pre-fluidized with most air for a long period, the minimum bubbling point can be identified using fresh, dry catalyst, fluidized with humidified air. (By weighing the catalyst before and after the cycle it can be established that there has been no significant increase in density of the particles during this relatively brief exposure to moist air.) In this experiment the measured gas velocity and bed expansion at minimum bubbling are found to be essentially the same as for fluidization of the dry catalyst with dry air, so the change in physical properties of the air is not the cause of the change in the minimum bubbling point. The remaining factors are the difference between the densities of dry and wet particles, and the difference between the contact forces. But the wet particles are measurably denser than the dry particles, and hydrodynamic criteria, such as (2), predict that the interval of uniform expansion will shrink as the density of the particles increases. This is the reverse of what we observe; the onset of bubbling is found be delayed to higher gas flows and larger bed expansions for the wet particles, relative to the dry particles. We must, therefore, conclude that it is the modification of surface conditions that is responsible for the significant difference between the minimum bubbling conditions observed with wet and dry catalyst, and the contention that the onset of bubbling is not influenced by changes in the contact force is incorrect.

Furthermore, the hydrodynamic stability condition of Foscolo & Gibilaro (1984) ((2) above), which is claimed to give reliable predictions of the void fraction at minimum bubbling over the whole range of fluid–particle systems, fails rather badly when compared with our observations. A test of this criterion is difficult for beds of cracking catalyst, because the uncertainty in the appropriate value for the particle density makes experimental values of the solid volume fraction uncertain to the extent of a multiplicative constant, even though accurate values of the bulk density can be measured. For the sand, on the other hand, the particle density is well defined, so a meaningful comparison of the observed and predicted void fractions at minimum bubbling is possible. Using a particle diameter of 154 μm, a particle density of 2620 kg/m$^3$, and the density and viscosity of dry air at ambient conditions, and estimating the terminal velocity $v_t$ by the well-known procedure of Kunii & Levenspiel (1977, chap. 3), with a particle sphericity factor of unity, the Foscolo–Gibilaro criterion gives $\epsilon_{mb} = 0.28$. This is smaller than the void fraction at minimum fluidization, so the criterion predicts that bubbling will begin immediately upon fluidization. However, from figure 25, the experiments show a bubble-free interval beyond minimum fluidization, and a void fraction of 0.38 at minimum bubbling. This observed value exceeds the estimate from (2) by 36%.

We believe the evidence adduced here, and elsewhere, is sufficient to dismiss hydrodynamic mechanisms as being responsible for the extended range of smooth expansion observed in the system we have studied, and to vindicate the view of Rietema

and co-workers (Rietema 1973; Rietema & Piepers 1990) that interparticle contact forces are the relevant physical phenomenon. However, we are not in complete agreement with their account of the transition from stability to instability. After noting the existence of yield stresses they propose that the elastic modulus of the particle assembly, in the interval of elastic behaviour between the yield limits, is large enough (see inequality (1) above) to stabilize the system against small disturbances. We agree. However, they go on to conclude that this modulus must decrease to a value corresponding to marginal (linear) stability as the bed is expanded to the minimum bubbling point. This is not necessary. Our experiments indicate that, within experimental accuracy, the elastic limits come together at the bed expansion corresponding to minimum bubbling; in other words, the *width* of the interval of elastic behaviour between the yield limits shrinks to zero just where bubbling begins. Within this interval the effective elastic modulus may remain large enough to maintain an ample margin of linear stability, right up to the bed expansion at which the elastic domain itself vanishes. What changes on expanding the bed toward the point of 'minimum bubbling' is then the *amplitude* of the disturbance needed to break the material out of the interval of elastic behaviour, and this amplitude shrinks to zero on approaching the minimum bubbling point.

There is further evidence for this view from the experiments in which the gas velocity was increased after the bed had been partially compacted, as shown in the segments aa′ and bb′ of figure 9. These start with the bed at the compressive yield limit and, as the gas flow is increased, they take it through the full width of the domain of elastic behaviour. Within this interval there is no measurable change at all in the bed height, as reflected by the fact that aa′ and bb′ are horizontal lines. For this to be the case, the effective elastic modulus must be very large. Furthermore, there is no detectable deviation from this behaviour when the starting point of the experiment is moved to higher bed expansions, so there is no indication of much decrease in the elastic modulus on moving toward the minimum bubbling point.

In summary, it is important to distinguish between the *stiffness* of the particle assembly within the domain of elastic behaviour, as measured by the elastic modulus, and the *strength* of the assembly, as measured by the stress needed to terminate elastic behaviour and induce plastic yield. Our experiments indicate that loss of strength, rather than loss of stiffness, is responsible for the loss of stability and consequent onset of bubbling.

We do not claim general applicability for the stabilizing mechanism observed here. The present work does not preclude the possibility that there are cases of smooth fluidization in which the stabilizing mechanism is hydrodynamic; it shows only that this is not so for the two particular cases studied. However, for solid particles fluidized by typical gases, solid–solid contacts occur very easily and it is not unlikely that they may provide the stabilizing mechanism in most, if not all cases. If hydrodynamic stabilization occurs, we believe it is most likely to be found in liquid fluidized beds of small particles, where the density of the particles is not much greater than that of the fluid. These would merit serious experimental study, taking great care to discriminate properly between stable and unstable beds, rather than merely assuming stability for all beds that do not bubble visibly.

This work was supported by the National Science Foundation, grant no. CTS-9006226. Thanks are due to Shell Development Company for providing the cracking catalyst used in most of the experiments, and for performing the size analyses reported in figure 3.

## REFERENCES

ABRAHAMSEN, A. R. & GELDART, D. 1980 Behavior of gas fluidized beds of fine powders. Part I. Homogeneous expansion. *Powder Technol.* **26**, 35–46.

ANDERSON, T. B. & JACKSON, R. 1968 Fluid mechanical description of fluidized beds. Stability of the state of uniform fluidization. *Ind. Engng Chem. Fundam.* **7**, 12–21.

BATCHELOR, G. K. 1988 A new theory of the instability of a uniform fluidized bed. *J. Fluid Mech.* **193**, 75–110.

EL-KAISSY, M. M. & HOMSY, G. M. 1976 Instability waves and the origin of bubbles in fluidized beds. *Intl J. Multiphase Flow* **2**, 379–395.

FOSCOLO, P. U. & GIBILARO, L. G. 1984 A fully predictive criterion for the transition between particulate and aggregative fluidization. *Chem. Engng Sci.* **39**, 1667–1675.

GARG, S. K. & PRITCHETT, J. W. 1975 Dynamics of gas fluidized beds. *J. Appl. Phys.* **46**, 4493–4500.

GELDART, D. 1973 Types of gas fluidization. *Powder Technol.* **7**, 285–292.

HAM, J. M., THOMAS, S., GUAZZELLI, E., HOMSY, G. M. & ANSELMET, M.-C. 1990 An experimental study of the stability of liquid fluidized beds. *Intl. J. Multiphase Flow* **16**, 171–185.

HOMSY, G. M., EL-KAISSY, M. M. & DIDWANIA, A. 1980 Instability waves and the origin of bubbles in fluidized beds. Part 2. Comparison with theory. *Intl. J. Multiphase Flow* **6**, 305–318.

JACKSON, R. 1963 The mechanics of fluidized beds. *Trans. Inst. Chem. Engrs* **41**, 13–28.

JANSSEN, H. A. 1895 Versuche uber getreidedruck in silozellen. *Ver. Deutsch. Ing. Zeit.* **39**, 1045–1049.

KUNII, D. & LEVENSPIEL, O. 1969 *Fluidization Engineering*, 1st edn. Wiley.

MEDLIN, J. & JACKSON, R. 1975 Fluid mechanical description of fluidized beds. The effect of distributor thickness on convective instabilities. *Ind. Engng Chem. Fundam.* **14**, 315–321.

MEDLIN, J., WONG, H. W. & JACKSON, R. 1974 Fluid Mechanical description of fluidized beds. Convective instabilities in bounded beds. *Ind. Engng Chem. Fundam.* **13**, 247–259.

MUTSERS, S. M. P. & RIETEMA, K. 1977*a* The effect of inter-particle forces on the expansion of a homogeneous gas fluidized bed. *Powder Technol.* **18**, 239–248.

MUTSERS, S. M. P. & RIETEMA, K. 1977*b* Gas–solids fluids fluidization in a centrifugal field. The effect of gravity upon bed expansion. *Powder Technol.* **18**, 249–256.

RICHARDSON, J. F. & ZAKI, W. N. 1954 Sedimentation and fluidization. *Trans. Inst. Chem. Engrs* **32**, 35–53.

RIETEMA, K. 1973 The effect of interparticle forces on the expansion of a homogeneous gas-fluidized bed. *Chem. Engng Sci.* **28**, 1493–1497.

RIETEMA, K. & PIEPERS, H. W. 1990 The effect of interparticle forces on the stability of gas-fluidized beds – I. Experimental evidence. *Chem. Engng Sci.* **45**, 1627–1639.

TSINONTIDES, S. C. 1992 A theoretical and experimental investigation of the mechanics of fluidized gas–particle systems. Ph.D. dissertation, Princeton University.

VERLOOP, J. & HEERTJES, P. M. 1970 Shock waves as a criterion for the transition from homogeneous to heterogeneous fluidization. *Chem. Engng. Sci.* **25**, 825–832.

WALLIS, G. B. 1969 *One-Dimensional Two-Phase Flow*. McGraw-Hill.